

UNIVERSITE KASDI MERBAH OUARGLA

Faculté des Sciences Appliquées  
Département de Génie Electrique



Mémoire

MASTER ACADEMIQUE

Domaine : Sciences et technologies

Filière : Electrotechnique

Spécialité : Réseaux électriques

Présenté par :

Larafi Tarek      Ouanis Aicha

**Thème:**

Recent meta-heuristic algorithm for solving  
combined heat and power dynamic economic  
dispatch

Soumis au jury composé de :

M <sup>f</sup> Benbouza Naima	MAA	Président	UKM Ouargla
M <sup>f</sup> Benyekhlef Larouci	MCB	Encadreur/rapporteur	UKM Ouargla
M <sup>f</sup> Kherfane Riad Lakhdar	MCB	Examineur	UKM Ouargla

Année universitaire 2021/2022

بِسْمِ اللَّهِ الرَّحْمَنِ الرَّحِيمِ

# *Acknowledgements*

*Praise be to God, who enabled us to complete this humble work,*

*Then all thanks and respect to our teacher, Mr. Larouci Benyekhlef for framing and guiding us*

*We also thank the members of the jury and do not forget our former professors since we joined the university*

*We thank everyone who contributed to this work, even with a kind word*



# *Dedication*

*I dedicate this humble work to everyone who has supported me financially and with care from near or far.*

*To the most precious thing I have to those who have stood by me all my life to my mother and my father AHMED.*

*To my only sister and my special brothers: MAROUAN – SOUHAIB – OMAR and The little Prince ANAS.*

*To my precious grandfather EL HADJ, may Allah have mercy on him.*

*And To all my big family: LARAFI*

*And to all my dear friends: AHMED-ABDEL RAHMAN-NADJI-AISSA-ABD EL DJABBAR-SALEM-IBRAHIM...*

*And to all the friends I didn't mention.*

*And to everyone who was the reason I succeeded from primary to college.*



☆ LARAFI TAREK ☆



# *Dedication*

*Praise be to God, who has not completed any effort or completed a quest except by His grace, and the servant has not overcome obstacles and difficulties without His success and assistance. To whom I prefer it to myself, and why not, because she sacrificed for me and spared no effort to make me always happy (my beloved mother)*

*We walk in the paths of life, and the one who controls our fates remains in every path we take, the one with a good face and good deeds, and he did not sting me throughout his life (Abi Aziz)*

*To a cloud that misleads me and waters me without desire, my coldness to its beautiful (dear brothers) and to (young family) may God protect them*

*To all the friends who helped me in my academic journey*



# Tables List

## Chapter III

<b>Tableau III.1:</b> Simulation results of fuel cost .....	<b>40</b>
<b>Tableau III.2:</b> Comparison results of fuel cost .....	<b>40</b>
<b>Tableau III.3:</b> Simulation results of fuel emission .....	<b>42</b>
<b>Tableau III.4:</b> Comparison results of fuel emission .....	<b>42</b>
<b>Tableau III.5:</b> Simulation results of CHP fuel cost .....	<b>44</b>
<b>Tableau III.6:</b> Simulation results of CHPEED .....	<b>46</b>

# List of Figures

## Chapter I

<b>Figure I.1:</b> The CHEED system.....	4
<b>Figure I.2:</b> Feasible operation region for a cogeneration unit .....	5
<b>Figure I.3:</b> valve point loading effect .....	6

## Chapter II

<b>Figure II.3:</b> Water molecules and their composition.....	14
<b>Figure II.4:</b> L-J potential curve.....	15
<b>Figure II.5:</b> Force curve of atoms .....	17
<b>Figure II.6 :</b> Function behaviors of $F'$ with different values of $\eta$ .....	18
<b>Figure II.5 :</b> Forces of an atom system with $KBest$ for $K = 5$ .....	21
<b>Figure II.6 :</b> Swarm motion of 5 atoms around a target in a 3-D space.....	22
<b>Figure II.7 :</b> Motion histories of 5 atoms during 50 iterations.....	22
<b>Figure II.8 :</b> Pseudo code of ASO algorithm .....	23
<b>Figure II.9 :</b> Crack propagation model in thin plates .....	26
<b>Figure II.10 :</b> Local figure with 30% of global size figure and some iterations.....	27
<b>Figure II.11 :</b> Pseudo code of the Transition procedure, corresponding to the Transition from larvae to adult state phase in the Mexican Axolotl Optimization (MAO) algorithm .....	29
<b>Figure II.12:</b> Pseudo code of the Accidents procedure, corresponding to the Injury and restoration state phase in the MAO algorithm.....	31
<b>Figure II.13 :</b> Pseudo code of the New Life procedure, corresponding to the Reproduction and Assortment phase in the MAO algorithm of the proposed Mexican Axolotl Optimization .....	32
<b>Figure II.17 :</b> Reproduction in the MAO. (a) Male parent, (b) female parent,(c) random number generated to uniformly distribute the parents' information, and (d) the resulting offspring.....	32
<b>Figure II.15 :</b> Pseudo code of the proposed Mexican Axolotl Optimization.....	34

## **Chapter III**

<b>Figure III.8:</b> Heat-power feasible operating region for the CHP unit 2 of test system 2.....	<b>38</b>
<b>Figure III.2:</b> Heat-power feasible operating region for the CHP unit 3 of test system 2.....	<b>38</b>
<b>Figure III.3:</b> Convergence Curve of Costs.....	<b>40</b>
<b>Figure III.4:</b> Run Number of Costs .....	<b>41</b>
<b>Figure III.5:</b> Convergence Curve of Emissions.....	<b>43</b>
<b>Figure III.6:</b> Run Number of Emissions .....	<b>43</b>
<b>Figure III.7:</b> Convergence Curve of CHP Costs.....	<b>45</b>
<b>Figure III.8:</b> Run Number of CHP Costs .....	<b>45</b>
<b>Figure III.9:</b> Convergence Curve of CHPEED Costs .....	<b>47</b>
<b>Figure III.10:</b> Run Number of CHPEED Costs .....	<b>47</b>

## List of Acronyms and Symbols

### Acronyms

**LA:** Lichtenberg algorithm

**EO:** Equilibrium Optimizer

**MAO:** Mexican Axolotl Optimization

**ASO:** Atom search optimization

**PSO:** particle swarm optimization

**MPSO:** Modified particle swarm optimization

**IPSO:** improved particle swarm optimization

**TAC – PSO:** time-varying acceleration particle swarm optimization

**DE:** Differential Evolution

**CHP:** Combined Heat and Power

**CEED:** Combined Economic Emission Dispatch

**CHPED:** Combined Heat and Power Economic Dispatch

**CHPEED:** Combined Heat and Power Economic Emission Dispatch

**ED:** economic dispatch

**EED:** economic emission dispatch

**WECS:** wind energy conversion systems

**AIA:** Artificial immune algorithm

**BFO:** Bacteria foraging optimization

**ACO:** Ant colony optimization

**ABC:** Artificial bee colony

**BBO:** Biogeography based optimization

**GSA:** Gravitational search algorithm

**TLBO:** Teaching–learning based optimization



## Symbols

$E_i^{TU}(P_{i,t}^{TU})$ : represents the total emissions to produce  $P_{i,t}^{TU}$

$\alpha_i, \beta_i, \gamma_i, \eta_i$  and  $\delta_i$ : are the emission function coefficients of generator  $i$

$T, I, K$  and  $L$ : are the total scheduling interval

$\alpha_l, \beta_l$  and  $c_l$ : are the positive fuel cost coefficients of generator

$D$ : is the dimension of the search space

$\varepsilon$ : is the depth of the potential well that represents the strength of the interaction

$\sigma$ : is the length scale that denotes the collision diameter

$j$ : the atom exerts on the  $i$ th atom

$i$ : the atom is simply given

$N$ : is the total number of atoms in an atomic system

$b_{ij}$ : is the fixed bond length between the  $i$ th and  $j$ th atoms

$kth$ : constraint for a bond works between the  $ikth$  and  $jkth$  atoms

$G_i$ : from the stretch of a covalent bond between two atoms acted

$i$ th: atom can be written

$\lambda_k$ : is the Lagrangian multiplier associated with  $\theta_k$

$\eta(t)$ : is the depth function to adjust the repulsion region or attraction region

$\alpha$ : is the depth weight

$h_{min}$  and  $h_{max}$ : are the lower and the upper limits of  $h$

$i$ : the atom from the other atoms can be considered a total force

$rand_j$ : is a random number in  $[0,1]$

$x_{best}(t)$ : is the position of the best atom at the  $t$ th iteration

$b_{i,best}$ : is a fixed bond length between the  $i$ th atom and the best atom

$\lambda(t)$ : is the Lagrangian multiplier

$\beta$ : is the multiplier weight

$m_i(t)$ : is the mass of the  $i$ th atom at the  $t$ th iteration

$K$ : gradually decreases with the lapse of iterations

$\lambda$  : be a transition parameter in  $[0,1]$  for the male axolotl  $m_j$

$m_{best}$  : be the best adapted male (the one with best value of the objective function  $O$ )

$f_{best}$ : is the best female

$f_i$  is the current female axolotl

$Q$ : is the volumetric flow rate into and out of the control volume

$C_{eq}$ : represents the concentration at an equilibrium state in which there is no generation inside the control volume

$G$  : is the mass generation rate inside the control volume

$V dC$ : reaches to zero

$Q V$ : represents the inverse of the residence time

$t_0$  and  $C_0$  : are the initial start time and concentration

## TABLE OF CONTENTS

Tables List .....	I
List of Figures .....	II
List of Acronyms and Symbols.....	IV
General Introduction .....	1
<b>Chapter I. Combined Heat Emission Economic Dispatch (CHEED)</b>	
I.1 Introduction .....	3
I.2 Mathematical Model.....	4
I.2.1 Problem Formulation of CHEED.....	4
I.3 Combined Heat and Power Dynamic Economic Emission Dispatch Model.....	5
I.3.1 Economic dispatch .....	5
I.3.2 Emission dispatch.....	6
I.3.3 Heat dispatch .....	6
I.3.4 Combined Economic Emission Dispatch .....	6
I.3.5 Combined Heat and Power CHP .....	7
I.3.6 Combined Economic Emission Heat dispatch .....	7
I.3.7 Constraints .....	8
I.4 Conclusion .....	10
<b>Chapter II. Meta heuristic Method</b>	
II.1 Introduction .....	12
II.2 Atom search optimization (ASO) .....	13
II.2.1 Basic molecular dynamics.....	13
II.2.2 Mathematical representation of interaction force .....	16
II.2.3 Mathematical representation of geometric constraint.....	19
II.2.4 Mathematical representation of atomic motion .....	20

---

---

*TABLE OF CONTENTS*

---

II.2.5 Framework of ASO algorithm .....	23
II.3 Backgrounds .....	25
II.3.1 Structural health monitoring.....	25
II.3.2 Crack tip formulation in thin plates .....	25
II.3.3 Lichtenberg algorithm .....	26
II.4 Mexican Axolotl Variable Optimization .....	28
II.4.1 The Axolotl in Nature.....	28
II.4.2 The Artificial Axolotl .....	28
II.5 Equilibrium optimizer .....	34
II.5.1 Inspiration.....	34
II.6 Conclusion.....	35

**Chapter III. Simulations and Results**

III.1 Introduction.....	37
III.2 Case 1 .....	39
III.3 Case 2 .....	41
III.4 Case 3 .....	44
III.5 Case 4 .....	46
III.6 Conclusion and future work.....	48
General conclusion.....	49
References .....	50

---

# General Introduction

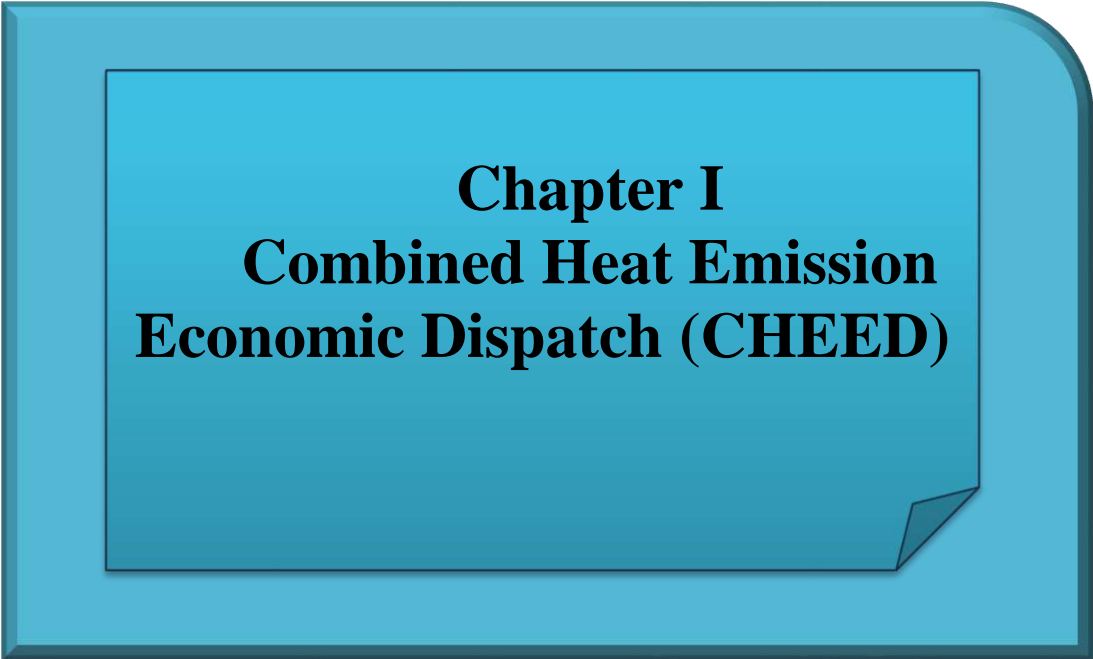
## ➤ Problem

Energy and heat are the basics of daily life. But the problem lies in how to exploit this energy as much as possible from its generation to its distribution until its exploitation, and that is proportional to reducing costs in a direct proportion, in addition to this problem trying to reduce the emissions caused.

In this work, the Combined Heat and Power Dynamic Economic Emissions Dispatch (CHPDEED) problem formulation is considered. This problem is a complicated nonlinear mathematical formulation with multiple, conflicting objective functions.

## ↳ Objective

- ✚ Energy and heat are combined through the CHP system to obtain the best possible solutions and the best results to reduce fuel cost, reduce emissions and increase the volume of energy utilized.
- ✚ The aim of this mathematical problem is to obtain the optimal quantities of heat and power output for the committed generating units which includes power and heat only units.
- ✚ The metaheuristics methods Lichtenberg algorithm (LA), Equilibrium optimizer (EO), Mexican axolotl optimization (MAO), Atom search optimization (ASO), Particle swarm optimization (PSO), Modified particle swarm optimization (MPSO) and improved particle swarm optimization (IPSO) are using to resolve the Combined Heat and Power Dynamic Economic Emissions Dispatch (CHPDEED) problem.
- ✚ The solutions of our approach that we will study through those algorithms are compared with the results available in the literature. We try to improve performance in proposal method in saving fuel costs and reducing emission levels compared to current methods.



**Chapter I**  
**Combined Heat Emission**  
**Economic Dispatch (CHEED)**

## I.1 Introduction

What is CHP? CHP is a technology that produces electricity and thermal energy at high efficiencies using a range of technologies and fuels. With on-site power production, losses are minimized and heat that would otherwise be wasted is applied to facility loads in the form of process heating, steam, hot water, or even chilled water. CHP can be located at an individual facility or building or it can be a district energy, micro grid, and/or utility resource that provides power and thermal energy to multiple end-users. CHP equipment can provide resilient power 24/7 in the event of grid outages, and it can be paired with other distributed energy technologies like solar photovoltaics (PV) and energy storage. In contrast to the production of energy alone, the output of these two outputs" energy and heat" greatly increases the efficiency of the CHP units the efficiency of CHP units is about 90% while conventional units are only about 60%. CHP's efficiency benefits result in reduced Primary energy which is the fuel that is consumed to create heat and/or electricity use and thus lower CO<sub>2</sub> emissions. An added advantage of CHP units over conventional units is that CHP units also yield lower emissions by about 13–18% [1].

Benefits of CHP include:

- **Efficiency benefits:** CHP requires less fuel than SHP (separate heat and power) to produce a given energy output, and because electricity is generated at the point of use, transmission and distribution losses that occur when electricity travels over power lines from central power plants are displaced.
- **Reliability benefits:** CHP can be designed to provide high-quality electricity and thermal energy on site, reducing reliance on the electric grid, decreasing the impact of outages, and improving power quality for sensitive equipment.
- **Environmental benefits:** Because less fuel is burned to produce each unit of energy output, CHP reduces emissions of greenhouse gases (GHG) and other air pollutants.
- **Economic benefits:** Because of its efficiency benefits, CHP can help facilities save money on energy. Also, CHP can provide a hedge against fluctuations in electricity costs[1].

As a research hotspot in the field of power system optimization, some progress has been reported on solving the EED problems incorporating renewable energy resources in recent years. In [2], the multi-objective economic emission dispatch problem is considered, which combines heat and wind power generation in a large micro-grid (MG), These reports describe the EED model considering renewable energy resources in detail, and various optimization strategies are utilized. Since there exist a number of EED problem types with renewable energy, most studies only consider one type of EED model, and the proposed methods may be difficult to apply to other kind of models. It is therefore meaningful to consider multiple types of EED models with different renewable energy sources. Under this consideration, this paper will investigate three different types of EED problems integrated renewable energy resources [2].

## I.2 Mathematical Model

This model mainly focuses on three different environmental economic dispatch models considering renewable sources, including the combined heat, emission, and economic dispatch (CHEED), and applies with renewable energy and combined emission economic dispatch problems with wind and PV penetration. The overall dispatching frameworks of the first model are shown in figure I. 1[2].

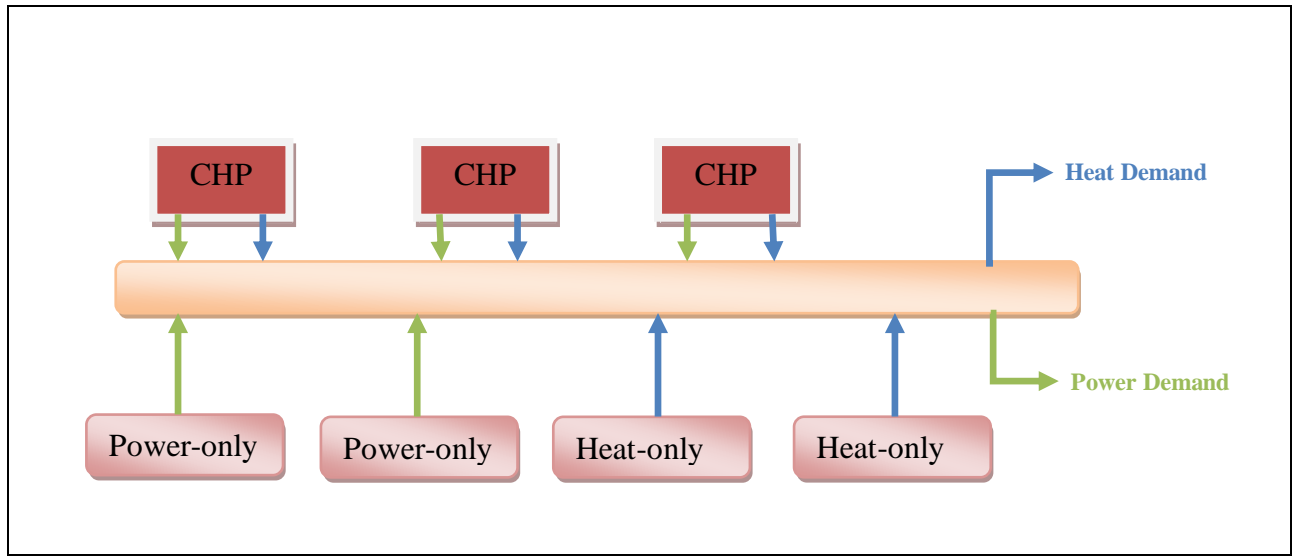


**Fig I.1:** The CHEED system.

### I.2.1 Problem Formulation of CHEED

The system considered in this paper contains conventional generators, cogeneration units, and heat-only units. The feasible operating region (FOR) of the cogeneration units is illustrated in figure I.2 [15], which is enclosed by the boundary curve ABCDEF. For the CHEED problem, the power is derived from the thermal units and cogeneration units while the heat is derived from cogeneration units and heat-only units. Under the condition of ensuring the power balance of the system and satisfying the constraints, the output of each unit is reasonably allocated to achieve the goal of minimizing the cost of heat and power production while minimizing the emission level. Thus, CHEED can be mathematically elaborated as follows[2].



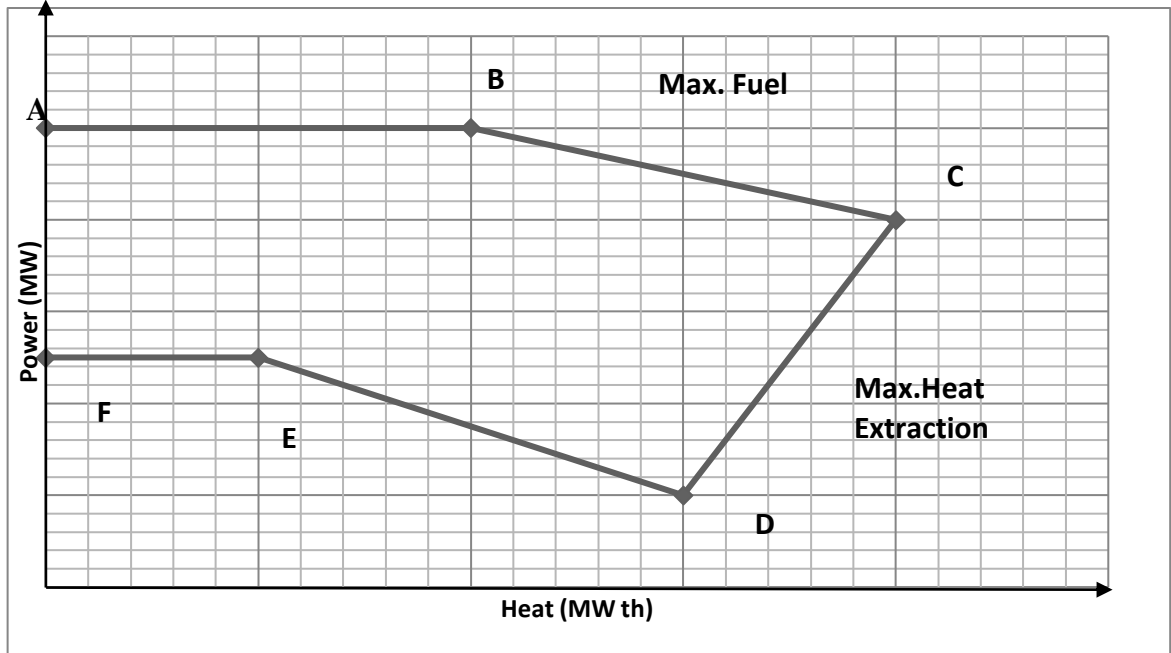


**Fig I.2:** Feasible operation region for a cogeneration unit.

### I.3 Combined Heat and Power Dynamic Economic Emission Dispatch Model

The CHPDEED mathematical model is made up of three distinct types of generators. They include: conventional thermal units (TU), CHP units, and heat-only units (H). Conventional thermal units and CHP units produce electric power whilst heat only units and CHP units produce heat. The CHPDEED mathematical problem has its objective as the minimization of the fuel costs and emissions of all units whilst satisfying the power and heat demand over the scheduling horizon under practical system constraints. The individual fuel cost and emissions objective functions of all three types of generating units (thermal, CHP and heat) are detailed [3].

#### I.3.1 Economic dispatch

The most common fuel function for thermal units is the quadratic representation. A more accurate representation is one that incorporates valve point effects given as:

$$C_i(P_{i,t}^{TU}) = \alpha_i + b_i P_{i,t}^{TU} + C_i (P_{i,t}^{TU})^2 + e_i \sin(f_i (P_{i,min}^{TU} - P_{i,t}^{TU})) \quad (I.1)$$

Where:

$\alpha_i$ ,  $b_i$  and  $C_i$  are the positive fuel cost coefficients of generator  $i$  respectively;

$e_i$  and  $f_i$  are the fuel cost coefficients representing valve point effects of generator  $i$ , respectively;

$P_{i,t}^{TU}$ : represents the power generated from thermal unit  $i$  at time  $t$ ;

$P_{i,min}^{TU}$ : represents the minimum capacity of thermal unit  $i$ ;

$C_i(P_{i,t}^{TU})$ : represents the fuel cost of producing  $P_{i,t}^{TU}$  [3].

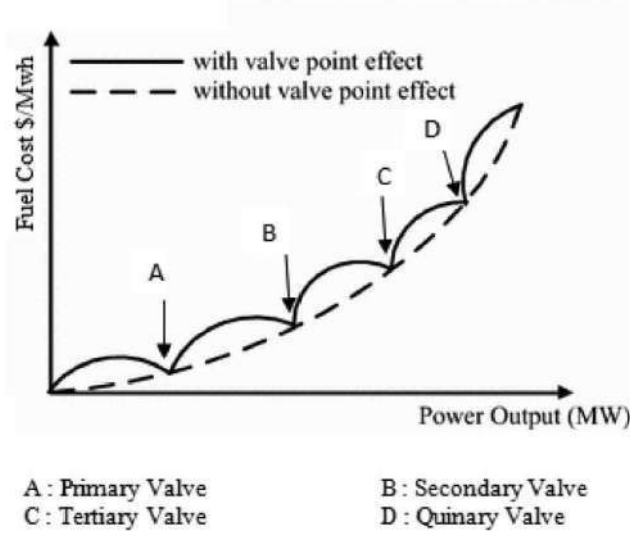


**Fig I.3:** Valve point loading effect.

### I.3.2 Emission dispatch

The emissions of thermal units are given by:

$$E_i^{TU}(P_{i,t}^{TU}) = \alpha_i + \beta_i P_{i,t}^{TU} + \gamma_i (P_{i,t}^{TU})^2 + \eta_i \exp(\delta_i P_{i,t}^{TU}) \quad (I.2)$$

This emission mathematical function is a combined quadratic and exponential representation of the thermal units power output.  $\alpha_i, \beta_i, \gamma_i, \eta_i$  and  $\delta_i$  are the emission function coefficients of generator  $i$  and  $E_i^{TU}(P_{i,t}^{TU})$  represents the total emissions to produce  $P_{i,t}^{TU}$  [3].

### I.3.3 Heat dispatch

These units produce only heat and the fuel cost function is depicted by:

$$C_l^H(H_{l,t}^H) = a_l + b_l H_{l,t}^H + c_l (H_{l,t}^H)^2 \quad (I.3)$$

Were:

$H_{l,t}^H$  denotes the total system heat demand.

### I.3.4 Combined Economic Emission Dispatch

The total fuel cost (for thermal, CHP and heat units) is given by:

$$C(PH) = \sum_{t=1}^T (\sum_{i=1}^I E_i^{TU}(P_{i,t}^{TU}) + \sum_{k=1}^K E_k^{CHP}(P_{k,t}^{CHP}, H_{k,t}^{CHP}) + \sum_{l=1}^L C_l^H(H_{l,t}^H)) \quad (I.4)$$

Where:

$T, I, K$  and  $L$  are the total scheduling interval, total number of thermal units, total number of CHP units, and total number of heat units, respectively.

In a similar manner, the total emission function (for thermal, CHP and heat units) is given by:

$$E(PH) = \sum_{i=1}^T (\sum_{i=1}^I E_i^{TU}(P_{i,t}^{TU}) + \sum_{k=1}^K E_k^{CHP}(P_{k,t}^{CHP}) + \sum_{i=1}^L E_i^H(H_{i,t}^H)) \quad (I.5)$$

Where:

$T, I, K$  and  $L$  are the total scheduling interval, total number of thermal units, total number of CHP units, and total number of heat units, respectively[3].

### I.3.5 Combined Heat and Power CHP

The CHP unit produces both power and heat. Thus, the fuel cost is a product of both outputs. This is usually represented as a convex cost function given as

$$C_k^{CHP}(P_{k,t}^{CHP}, H_{k,t}^{CHP}) = a_k + b_k P_{k,t}^{CHP} + c_k (P_{k,t}^{CHP})^2 + d_k H_{k,t}^{CHP} + e_k (H_{k,t}^{CHP})^2 + f_k (P_{k,t}^{CHP}, H_{k,t}^{CHP}) \quad (I.6)$$

Where:

$a_k, b_k, c_k, d_k, e_k$  and  $f_k$  are the fuel cost coefficients of CHP generator  $l$  respectively;

$C_k^{CHP}(P_{k,t}^{CHP}, H_{k,t}^{CHP})$ : is the fuel cost for CHP generator  $l$  to produce heat and power  $(P_{k,t}^{CHP}, H_{k,t}^{CHP})$ .

The total CHP unit emissions are solely a function of the power generated and is given as:

$$C_k^{CHP}(P_{k,t}^{CHP}) = (\alpha_k + \beta_k) P_{k,t}^{CHP} \quad (I.7)$$

Where:

$\alpha_k$  and  $\beta_k$  are emission function coefficients[3].

### I.3.6 Combined Economic Emission Heat dispatch

Where:

$\alpha_l, \beta_l$  and  $c_l$  are the positive fuel cost coefficients of generator  $l$ , respectively; the emission function similarly is given by:

$$E_l^H(H_{l,t}^H) = (\alpha_l + \beta_l) H_{l,t}^H \quad (I.8)$$

Where  $\alpha_i$  and  $\beta_i$  are the emissions coefficients of heat units  $l$ [3].

### I.3.7 Constraints

The constraints for the CHPDEED problem's objective function (Equations (I.4) and (I.5)) are given below [3]:

$$\sum_{i=1}^I P_{i,t}^{TU} + \sum_{k=t}^K P_{k,t}^{CHP} = D_t + loss_t \quad (I.9)$$

$$\sum_{k=1}^K H_{k,t}^{CHP} + \sum_{l=1}^L H_{l,t}^H = HD_t + loss_t \quad (I.10)$$

$$P_{i,min}^{TU} \leq P_{i,t}^{TU} \leq P_{i,max}^{TU} \quad (I.11)$$

$$P_{k,min}^{CHP}(H_{k,t}^{CHP}) \leq P_{k,t}^{CHP} \leq P_{k,max}^{CHP}(H_{k,t}^{CHP}) \quad (I.12)$$

$$H_{k,min}^{CHP}(P_{k,t}^{CHP}) \leq H_{k,t}^{CHP} \leq H_{k,max}^{CHP}(P_{k,t}^{CHP}) \quad (I.13)$$

$$H_{i,min}^H \leq H_{i,t}^H \leq H_{i,max}^H \quad (I.14)$$

$$DR_i^{TU} < P_{i,t+1}^{TU} - P_{i,t}^{TU} < UR_i^{TU} \quad (I.15)$$

$$DR_k^{CHP} < P_{k,t+1}^{CHP} - P_{k,t}^{CHP} < UR_k^{CHP} \quad (I.16)$$

Where:

$$loss_t = \sum_{i=1}^I \sum_{z=1}^Z P_{i,t} B_{i,z} P_{z,t} \quad (I.17)$$

$P_{i,t}^{TU}$ : is the power generated from thermal generator  $i$  at time  $t$ ;

$P_{k,t}^{CHP}$ : is the power generated from CHP generator  $k$  at time  $t$ ;

$H_{k,t}^{CHP}$ : is the heat produced from CHP generator  $k$  at time  $t$ ;

$H_{l,t}^H$ : is the heat produced from heat generator  $l$  at time  $t$ ;

$D_t$ : is the total system power demand at time  $t$ ;

$HD_t$ : is the total system heat demand at time  $t$ ;

$loss_t$ : is the total system loss at time  $t$ ;

$P_{i,min}^{TU}$  and  $P_{i,max}^{TU}$ : is the minimum and maximum power capacity of thermal generator  $i$  respectively;

$H_{l,min}^H$  and  $H_{l,max}^H$ : are the minimum and maximum heat capacities of generator  $l$  respectively;

$P_{k,min}^{CHP}(H_{k,t}^{CHP})$  and  $H_{k,max}^{CHP}(H_{k,t}^{CHP})$ : are the minimum and maximum power capacities of CHP generator  $k$ , respectively. Both parameters are functions of the heat produced ( $H_{k,t}^{CHP}$ )

$H_{k,min}^{CHP}(P_{k,t}^{CHP})$  and  $H_{k,max}^{CHP}(P_{k,t}^{CHP})$ : are the minimum and maximum heat capacities of CHP generator  $k$ , respectively. Both parameters are functions of the power produced ( $P_{k,t}^{CHP}$ )

$DR_i^{TU}$  and  $UR_i^{TU}$ : are the maximum ramps down and up rates of thermal generator  $i$ , respectively;

$DR_k^{CHP}$  and  $UR_k^{CHP}$ : are the maximum ramps down and up rates of CHP generator  $k$ , respectively;

$B_{i,z}$ : is the  $iz$ Th element of the loss coefficient square matrix of size  $I + L$ ;

Equations (I.9)–(I.16) represent the constraints of the mathematical model and their interpretation is given as:

- Constraint (I.9) is termed the “power balance constraint”. Its role is to compel the total output power from both thermal and CHP units at each scheduling interval to satisfy the load demand and transmission line losses. Transmission line losses are determined by the B-coefficient method [3]. And is represented mathematically in (I.17).  $B_{i,z}$ : is the  $iz$ th element of the loss coefficient square matrix  $B$  of size  $I + L$ . This method has been used in [16-17].
- Constraint (I.10) is termed the “heat balance constraint” and its role is to compel the heat output from both CHP and heat-only units to match heat demand[3].
- The third constraint is the thermal generation limits constraint (I.11). It compels the output power from thermal generators to not exceed allowed limits
- The fourth constraint (I.12) limits power produced from CHP units within allowable units[3].
- The fifth constraint (I.13) limits heat produced from CHP units within allowable limits[3].
- Constraint (I.14) ensures that the heat produced from heat only units are within allowable limits[3].
- Constraint (I.15) is the “generator ramp rate limits constraint” for thermal generators and compels the thermal generators output power for consecutive scheduling intervals to be within allowable ramp rate limits[3].
- Constraint (I.16) is termed “generator ramp rate limits constraint” for CHP generators. Similar to constraint (I.15), it compels the output power for CHP units for consecutive scheduling intervals to be within allowable ramp rate limits [3].

The two objective functions (Equations (I.4) and (I.5)) can be concatenated into a single objective function via a weighting factor  $\omega$ . The resultant single objective function is still constrained by [3]:

$$\min[\omega * C(PH) + (1 - \omega)E(PH)] \quad (I.18)$$

Where:

$\omega$  and  $(1 - \omega)$  are weighting factors. The condition to be satisfied is [3]:

$$\omega + (1 - \omega) = 1 \quad (I.19)$$

Both weighting factors are non-negative and can be controlled by the modeler based on the preference given to objective functions. When the modeler seeks to minimize fuel costs alone then  $\omega = 1$  (CHPDED), however, when the modeler wants to minimize emissions alone then  $\omega = 0$  (CHPPDED), it is assumed for the purpose of this article that equal weights are given to both objective functions, thus  $\omega = (1 - \omega) = 0.5$ [3].

## **I.4 Conclusion**

In this chapter, we reviewed a problem of the independent production of both power and heat, which incurs significant economic and environmental losses we presented a definition of the system of combining them (CHP) and improve.

And we will proceed to work with recent meta heuristic algorithm for solving combined heat and power dynamic economic dispatch such as: Lichtenberg algorithm (LA), Equilibrium optimizer (EO), Mexican axolotl optimization (MAO), Atom search optimization (ASO), Particle swarm optimization (PSO), Modified particle swarm optimization (MPSO) and improved particle swarm optimization (IPSO).



**Chapter II**  
**Metaheuristic Method**

## II.1 Introduction

A majority of the real-life optimization problems in the area of engineering, science, economics, etc. involve different types of constraints. Moreover, these problems are of different characteristics such as linear, nonlinear, quadratic, polynomial, cubic, etc. The classical derivative-based optimization techniques often fail to solve such type of problems. Thus, the difficulties associated with these types of real-life optimization problems motivate to develop alternative and effective methods to solve it [4].

In the last decades, different MAs have been developed and used. For example Artificial immune algorithm (AIA) is inspired by the principle and mechanism of the immune system of living beings. Bacteria foraging optimization (BFO) mimics the social foraging behaviour of *Escherichia coli*. Particle swarm optimization (PSO) simulates the intelligent behaviour of a flock of migrating birds in search of their destination. Ant colony optimization (ACO) works on the principle of foraging behaviour of the ant for the food. Artificial bee colony (ABC) algorithm mimics the foraging behavior and information sharing ability of honey bee swarm. Biogeography based optimization (BBO) simulate the principle of immigration and emigration of the species from one place to the other [4]. Gravitational search algorithm (GSA) works on the principle of the law of gravity and mass interaction. Teaching–learning based optimization (TLBO) algorithm mimics the teaching–learning ability of teacher and learners in a class room. Evolutionary membrane algorithm simulates the structure and functioning of a biological living cell [4]. There is no question about the exploration capabilities, these algorithms holds, has been successfully applied to solve several different types of search and optimization problems. The successes of these algorithms are greatly based on the parameters they used basically guides the searching and are majorly contributing in the exploration and exploitation of the search space.

All these algorithms are population-based algorithms where a group of solutions carry out the search process. The search characteristics of different algorithms are based on various natural phenomena as explained above. Researchers reported the successful application of various algorithms for a wide variety of real-life applications [4]. However, the success of any meta heuristic optimization algorithms depends on how the algorithm balances the exploration and exploitation of the search process. Exploration is the process of abrupt movement in the search space to cover it entirely while exploitation is the process to refine certain areas of explored search space. Pure exploration enhances the capacity of any algorithm to produce new solutions with less precision. Conversely, pure exploitation increases the possibility of trapping at the local optimum solution during the search process. Therefore, a proper balance between exploration and exploitation is always required for a better performance of any search algorithm [4].

In this thesis, efforts have been put to resolve this issue to a certain extent in the proposed algorithms: Lichtenberg algorithm (LA), Equilibrium optimizer (EO), Mexican axolotl optimization (MAO), Atom search optimization (ASO), Particle swarm optimization (PSO), Modified particle swarm optimization (MPSO) and improved particle swarm optimization (IPSO).



## II.2 Atom search optimization (ASO)

In this section, a novel optimization algorithm named atom search optimization (ASO) that is inspired by molecular dynamics is introduced. In ASO, the position of each atom within the search space represents a solution measured by its mass, with a better solution indicating a heavier mass, and vice versa. All atoms in the population will attract or repel each other according to the distance among them, encouraging the lighter atoms to move towards the heavier ones. Heavier atoms have smaller acceleration, which makes them seek intensively for better solutions in local spaces. Lighter atoms have greater acceleration, which makes them search extensively to find new promising regions in the entire search space [5].

The general unconstrained optimization problems can be defined as:

$$\text{Minimize } f(x), x = (x^1, \dots, x^D) \quad (\text{II.1})$$

for

$$Lb \leq x \leq Ub, Lb = [lb^1, \dots, lb^D], Ub = [ub^1, \dots, ub^D] \quad (\text{II.2})$$

Where:

$dx^d (d = 1, \dots, D)$  is the  $d$ th component of the search space,  $lb^d$  and  $ub^d$  are the  $d$ th components of the lower and upper limits, respectively, and  $D$  is the dimension of the search space.

In order to solve this unconstrained optimization, suppose an atom population with  $N$  atoms. The position of the  $i$ th atom is expressed as:

$$x_i = [x_i^1, \dots, x_i^D], i = 1, \dots, N \quad (\text{II.3})$$

Where:

$x_i^d (d = 1, \dots, D)$  is the  $d$ th position component of the  $i$ th atom in a  $D$ -dimension space. In the initial iterations of ASO, each atom interacts with others by the attraction or the repulsion among them, and the repulsion can avoid the over-concentration of atoms and the premature convergence of the algorithm, thus enhancing the exploration ability in the entire search space. As iterations pass, the repulsion gradually weakens and the attraction gradually strengthens, which signifies that the exploration decreases and the exploitation increases. In the final iterations, each atom interacts with others just by the attraction, which ensures that the algorithm has a good exploitation capability [5].

### II.2.1 Basic molecular dynamics

ASO is inspired by basic molecular dynamics. From the micro perspective, a definition of "matter", based on its physical and chemical structure, is thus: matter is made up of molecules. A molecule is the smallest unit of a chemical compound, and it exhibits the same chemical properties as those of that specific compound. A molecule is composed of atoms held together by covalent bonds that vary greatly in terms of complexity and size. So all substances are made of atoms and all atoms have mass and volume. Figure II.1 shows the

composition of water molecules, each of which is made up of two hydrogen atoms and one oxygen atom, jointly held by two covalent bonds. For an atomic system, all the atoms interact and are in constant motion, whether in the state of gas, liquid or solid. They are very complex in terms of their structure and microscopic interactions. Because an atomic system is typically composed of numerous atoms, it is analytically impossible to determine their properties that are affected by factors such as temperature, pressure, and so on. With the development of computer technology, molecular dynamics (MD) has rapidly developed in recent years. It circumvents this problem with the use of a computer simulation method to examine the physical movements of atoms and molecules [5].

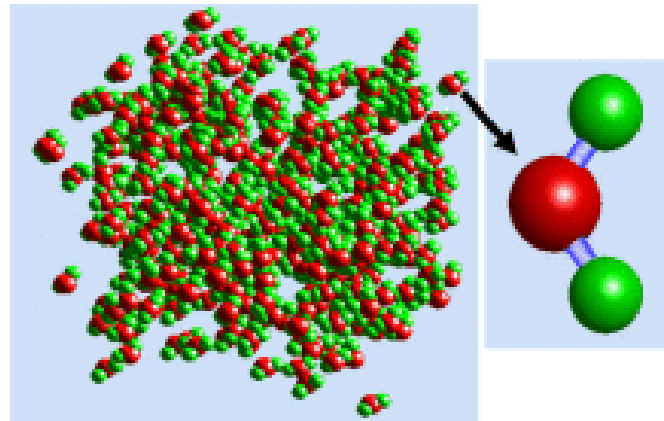


**Fig II.1:** Water molecules and their composition.

MD was initially conceived in the field of theoretical physics but its use has been extended to computational chemistry, materials science, and biology. Atomic motion follows the classical mechanics [16]. The interaction force among the atoms has two principal characteristics in an atom system. The first is the repulsion to compression, which repels at a close range of crowdedness. The second is the attraction that binds atoms together such as in solid and liquid states. Atoms attract each other over a further range of separation. The potential energy of atoms can well account for these two characteristics, and there are a wide variety of pair-wise formulas in the literature used to express the potential energy [17-18]. The Lenard-Jones (L-J) potential, initially proposed for liquid, is a simple mathematical model that approximates the interaction force between a pair of atoms [5]. The L-J potential between the  $i$ th and the  $j$ th atoms is commonly expressed as

$$U(r_{ij}) = 4\epsilon \left[ \left( \frac{\sigma}{r_{ij}} \right)^{12} - \left( \frac{\sigma}{r_{ij}} \right)^6 \right] \quad (\text{II.4})$$

Where:

$\epsilon$ : is the depth of the potential well that represents the strength of the interaction,  $\sigma$ : is the length scale that denotes the collision diameter,  $r_{ij} = x_j - x_i$ , and  $x_i(x_{i1}, x_{i2}, x_{i3})$ : is the position of the  $i$ th atom in a 3-D space, so the Euclidian distance between the  $i$ th and  $j$ th atoms is:

$$r_{ij} = \|x_j - x_i\| = \sqrt{(x_{i1} - x_{j1})^2 + (x_{i2} - x_{j2})^2 + (x_{i3} - x_{j3})^2} \quad (\text{II.5})$$

In equation (II.4),  $(\sigma/r)^{12}$  and  $(\sigma/r)^6$  represent the repulsive and attractive interactions, respectively. The L-J potential curve is illustrated in figure II.2, in which the attraction and repulsion regions are shown. In the repulsion region, the repulsion of the atoms rapidly increases as the distance between two atoms decreases. In the attraction region, as the distance between two atoms increases towards a certain further separation, the attraction gradually drops to zero. When two atoms reach an equilibration distance ( $r = 1.12\sigma$ ), their minimum bonding potential energy is reached. At this point, the interaction force between the atoms is equal to zero [5].

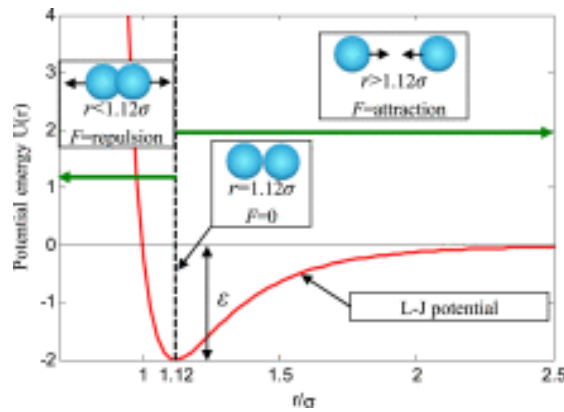


**Fig II.2:** L-J potential curve.

Having specified the potential energy function, the interaction force that the  $j$  th atom exerts on the  $i$ th atom is:

$$F_{ij} = -\nabla U(r_{ij}) = \frac{24\epsilon}{\sigma^2} \left[ \left( \frac{\sigma}{r_{ij}} \right)^{14} - \left( \frac{\sigma}{r_{ij}} \right)^8 \right] r_{ij} \quad (\text{II.6})$$

So the total interaction force exerted on the  $i$  th atom is simply given as:

$$F_i = \sum_{\substack{j=1 \\ j \neq i}}^N F_{ij} \quad (\text{II.7})$$

Where:

$N$ : is the total number of atoms in an atomic system.

To study more complex molecules, a molecular dynamics method with geometric constraints is proposed in [19], in which a combination of geometrical constraints and internal motion of atoms is considered. In polyatomic molecules, the highest-frequency internal vibrations are usually decoupled from rotational and translational motions. Thus a certain number of rigid bonds are introduced in the skeleton of the molecules. Consider the case in which the structure of a molecule is subject to one or more geometries. A constraint needs to be introduced to fix the distance between any two atoms with covalent bonds, and the mode can be expressed as.

$$|x_i - x_j|^2 = b_{ij}^2 \quad (\text{II.8})$$

Where:

$b_{ij}$  is the fixed bond length between the  $i$ th and  $j$ th atoms. Suppose that there are a total of  $l$  constraints influencing a particular molecule, And if the  $k$ th constraint for a bond works between the  $ik$ th and  $jk$ th atoms, then the  $k$ th constraint is:

$$\theta_k = |x_{ik} - x_{jk}|^2 - b_{ij}^2 = 0, k = 1, 2, \dots, l \quad (\text{II.9})$$

Hence, the constraint force  $G_i$  from the stretch of a covalent bond between two atoms acted on the  $i$ th atom can be written as:

$$G_i = -\sum_{k=1}^l \lambda_k \nabla_i \theta_k = -2 \sum_{k=1}^l \lambda_k (x_{ik} - x_{jk}) \quad (\text{II.10})$$

Where:

$\lambda_k$  is the Lagrangian multiplier associated with  $\theta_k$ . Hence, the motion equation of atoms with the constraint can be modified as:

$$F_i + G_i = m_i a_i \quad (\text{II.11})$$

For equation (II.11), the forces exerted on the atoms include not only all non-constraint interaction forces among molecules, but also the constraint force(s) within each molecule, thus embodying the essence of atomic motion. In summary, basic molecular dynamics describes the movement principles of atoms, including the characteristics of the potential function, the motion mode of atoms with a non-constraint interaction force, and a geometric constraint force. Despite the simplicity of the analytical model, the physics-based study of molecular dynamics can be used to determine thermodynamic properties of the system, and indeed presents opportunities for many theoretical studies and practical applications [5].

### II.2.2 Mathematical representation of interaction force

The interaction force resulting from the L-J potential is the priming power of atomic motion. The interaction force acted on the  $i$ th atom from the  $j$ th atom at the  $t$ th iteration in equation (II.6) can be rewritten as:

$$F_{ij}(t) = \frac{24\varepsilon(t)}{\sigma(t)} \left[ 2 \left( \frac{\sigma(t)}{r_{ij}(t)} \right)^{13} - \left( \frac{\sigma(t)}{r_{ij}(t)} \right)^7 \right] \frac{r_{ij}(t)}{r_{ij}^d(t)} \quad (\text{II.12})$$

And

$$F'_{ij}(t) = \frac{24\varepsilon(t)}{\sigma(t)} \left[ 2 \left( \frac{\sigma(t)}{r_{ij}(t)} \right)^{13} - \left( \frac{\sigma(t)}{r_{ij}(t)} \right)^7 \right] \quad (\text{II.13})$$

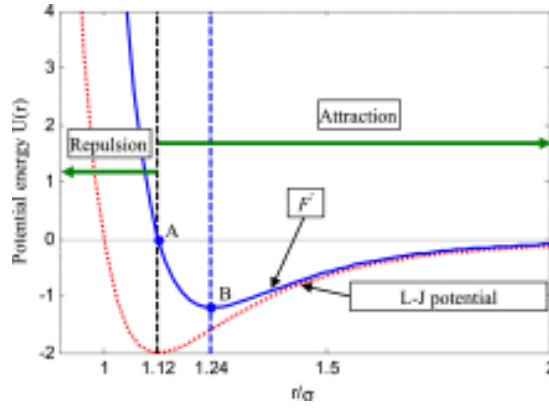


**Fig II.3:** Force curve of atoms.

The force curve of atoms is shown in figure II.3. As shown, the atoms keep a relative distance, varying in a certain range all the time from the repulsion or attraction, and the change amplitude of the repulsion relative to the equilibration distance ( $r = 1.12\sigma$ ) is much greater than that of the attraction. However, this model cannot be used directly to handle optimization problems, mainly because ASO needs to obtain more positive attraction and less negative repulsion as iterations increase, as shown in figure II.3, equation (II.13) cannot satisfy this point. Accordingly, a revised version of this equation is developed, as follows, to solve optimization problems [5].

$$F'_{ij}(t) = -\eta(t) \left[ 2(h_{ij}(t))^{13} - (h_{ij}(t))^7 \right] \quad (\text{II.14})$$

Where:

$\eta(t)$  :is the depth function to adjust the repulsion region or attraction region, which can be defined as:

$$\eta(t) = \alpha \left( 1 - \frac{t-1}{T} \right)^3 e^{-\frac{20t}{T}} \quad (\text{II.15})$$

Where:

$\alpha$  :is the depth weight and  $T$  is the maximum number of iterations. The function behaviors of  $F'$ , with different  $\eta$  corresponding to  $h$  ranging from 0.9 to 2, are illustrated in figure II.4. From the figure, the repulsion occurs when  $h$  ranges from 0.9 to 1.12, the attraction occur when  $h$  is between 1.12 and 2, and the equilibration occurs when  $h=1.12$ . The attraction gradually increases with the increase of  $h$  from the equilibration ( $h=1.12$ ), reaches a maximum ( $h=1.24$ ) and then begins to decrease. The attraction is approximately equal to zero when  $h$  is greater than or equal to 2. Therefore, in ASO, to improve the exploration, a lower limit of the repulsion with a smaller function value is set to  $h=1.1$  and an upper limit of attraction with a larger function value is set to  $h=1.24$ . Therefore,  $h$  is defined as [5]:

$$h_{ij}(t) = \begin{cases} h_{\min} & \frac{r_{ij}(t)}{\sigma(t)} < h_{\min} \\ \frac{r_{ij}(t)}{\sigma(t)} & h_{\min} \leq \frac{r_{ij}(t)}{\sigma(t)} \leq h_{\max} \\ h_{\max} & \frac{r_{ij}(t)}{\sigma(t)} > h_{\max} \end{cases} \quad (\text{II.16})$$

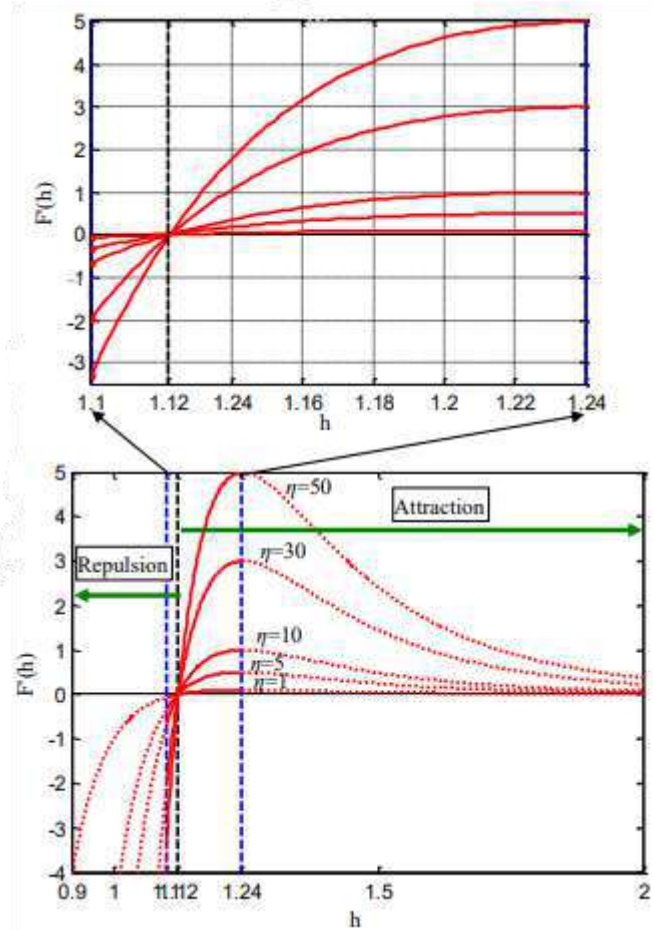


**Fig II.4:** Function behaviors of  $F'$  with different values of  $\eta$ .

Where:

$h_{\min}$  and  $h_{\max}$  are the lower and the upper limits of  $h$ , respectively, and the length scale  $\sigma(t)$  is defined as:

$$\sigma(t) = \left\| x_{ij}(t), \frac{\sum_{j \in K_{\text{best}}} x_{ij}(t)}{K(t)} \right\|_2 \quad (\text{II.17})$$

And

$$\begin{cases} h_{\min} = g_0 + g(t) \\ h_{\max} = u \end{cases} \quad (\text{II.18})$$

Where:

$Kbest$ , which is a subset of an atom population, is made up of the first  $K$  atoms with the best function fitness values. As a drift factor,  $g$  can make the algorithm drift from the exploration to the exploitation and is given as:

$$g(t) = 0.1 \times \sin\left(\frac{\pi}{2} \times \frac{t}{T}\right) \quad (\text{II.19})$$

Then the sum of components with random weights acted on the  $i$  th atom from the other atoms can be considered a total force, which is expressed as:

$$F_i^d(t) = \sum_{j \in Kbest} rand_j F_{ij}^d(t) \quad (\text{II.20})$$

Where:

$rand_j$  is a random number in  $[0,1]$  [5].

### II.2.3 Mathematical representation of geometric constraint

The geometric constraint in molecular dynamics plays an important role in atomic motion. For simplicity, suppose each atom in ASO has a covalence bond with the best atom [5]. Thus each atom is acted on by a constraint force from the best atom, so the constraint of the  $i$ th atom can be rewritten as:

$$\theta(t) = [ |x_i(t) - x_{best}(t)|^2 - b_{i,best}^2 ] \quad (\text{II.21})$$

Where:

$x_{best}(t)$  is the position of the best atom at the  $t$ th iteration, and  $b_{i,best}$  is a fixed bond length between the  $i$ th atom and the best atom. Hence the constraint force can be obtained as:

$$G_i^d(t) = -\lambda(t) \nabla \theta_i^d(t) = -2\lambda(t) (x_i^d(t) - x_{best}^d(t)) \quad (\text{II.22})$$

Where:

$\lambda(t)$  is the Lagrangian multiplier. Then, making the substitution of  $2\lambda \rightarrow \lambda$ , the constraint force can be redefined as:

$$G_i^d(t) \lambda(t) (x_i^d(t) - x_{best}^d(t)) \quad (\text{II.23})$$

The Lagrangian multiplier is defined as:

$$\lambda(t) = \beta e^{-\frac{20t}{T}} \quad (\text{II.24})$$

Where:

$\beta$ : is the multiplier weight.

### II.2.4 Mathematical representation of atomic motion

With the interaction force and the geometric constraint, the acceleration of the  $i$ th atom at time  $t$  can be written as:

$$a_i^d(t) = \frac{F_i^d(t)}{m_i^d(t)} + \frac{G_i^d(t)}{m_i^d(t)} = -\alpha \left(1 - \frac{t-1}{T}\right)^3 e^{-\frac{20t}{T}} \sum_{j \in K_{best}} \frac{\text{rand}_j [2 \times (h_{ij}(t))^{13} - (h_{ij})^7]}{m_i(t)} \quad (\text{II.25})$$

$$\frac{(x_j^d(t) - x_i^d(t))}{\|x_i(t), x_j(t)\|_2} + \beta e^{-\frac{20t}{T}} \frac{x_{best}^d(t) - x_i^d(t)}{m_i(t)}$$

Where:

$m_i(t)$  is the mass of the  $i$ th atom at the  $t$ th iteration, which can be measured at the simplest level by its function fitness value. The mass of the  $i$ th atom can be calculated as:

$$M_i(t) = e^{-\frac{F_{i,t}^i(t) - F_{best}^i(t)}{F_{worst}^i(t) - F_{best}^i(t)}} \quad (\text{II.26})$$

$$m_i(t) = \frac{M_i(t)}{\sum_{j=1}^N M_i(t)} \quad (\text{II.27})$$

$$Fit_{best}(t) = \min_{i \in \{1, 2, \dots, N\}} Fit_i(t) \quad (\text{II.28})$$

$$Fit_{wors}(t) = \max_{i \in \{1, 2, \dots, N\}} Fit_i(t) \quad (\text{II.29})$$

To simplify the algorithm, the position and velocity of the  $i$ th atom at the  $(t + 1)$ th iteration can be denoted as follows.

$$v_i^d(t + 1) = \text{rand}_i^d v_i^d(t) + a_i^d(t) \quad (\text{II.30})$$

$$x_i^d(t + 1) = x_i^d(t) + v_i^d(t + 1) \quad (\text{II.31})$$



In ASO algorithm, to enhance the exploration in the first stage of iterations, each atom needs to interact with as many atoms with better fitness values as its  $K$  neighbors. To enhance the exploitation in the final stage of iterations, the atoms need to interact with as few atoms with better fitness values as its  $K$  neighbors. Therefore, as a function of time,  $K$  gradually decreases with the lapse of iterations.  $K$  can be calculated as:

$$K(t) = N - (N - 2) \times \sqrt{\frac{t}{T}} \quad (\text{II.32})$$

The forces of an atom population are shown in figure II.5, in which the first 5 atoms with the best fitness values are regarded as the  $KBest$ . As shown in the figure,  $A_1, A_2, A_3$  and  $A_4$  compose the  $KBest$ .  $A_5, A_6$  and  $A_7$  attract or repel each atom in the  $KBest$ , and  $A_1, A_2, A_3$  and  $A_4$  attract or repel each other. Each atom in the population except for  $A_1$  ( $x_{best}$ ) has a constraint force from the best atom  $A_1$  [5].

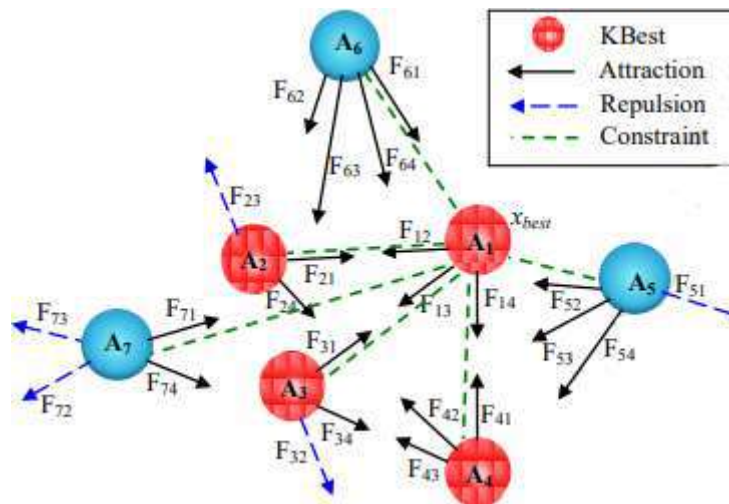


**Fig II.5:** Forces of an atom system with  $KBest$  for  $K = 5$ .

A simulation is conducted to examine how atoms move with this mathematical model. The swarm motion of 5 atoms around a target in a 3-D space is illustrated in figure II.6, in which 5 different colored balls represent 5 different atoms, and the red point represents the desired target that every atom wants to reach. Initially, the positions of the 5 atoms are randomly generated in the search space. With the lapse of time  $t$ , all the atoms gradually approach the target using the mathematical mode and form a swarm. Finally, all the atoms converge to the target. Additionally, it can be found that, although the green atom is far away from the swarm when  $t=20$ , the other atoms also pull it back by the attraction in the subsequent iterations, and all the atoms do not become too concentrated because of the repulsion. The motion histories of the 5 atoms during 50 iterations are illustrated in figure II.7 [5].

It is apparent that the atoms grow denser when they are closer to the target, and the distribution of atoms in the search space is sufficient to demonstrate that the model proposed can achieve the transition from the exploration for the entire search space to the exploration for a focused region. It is obvious that this search characteristic can be extended to a n-D space [5].

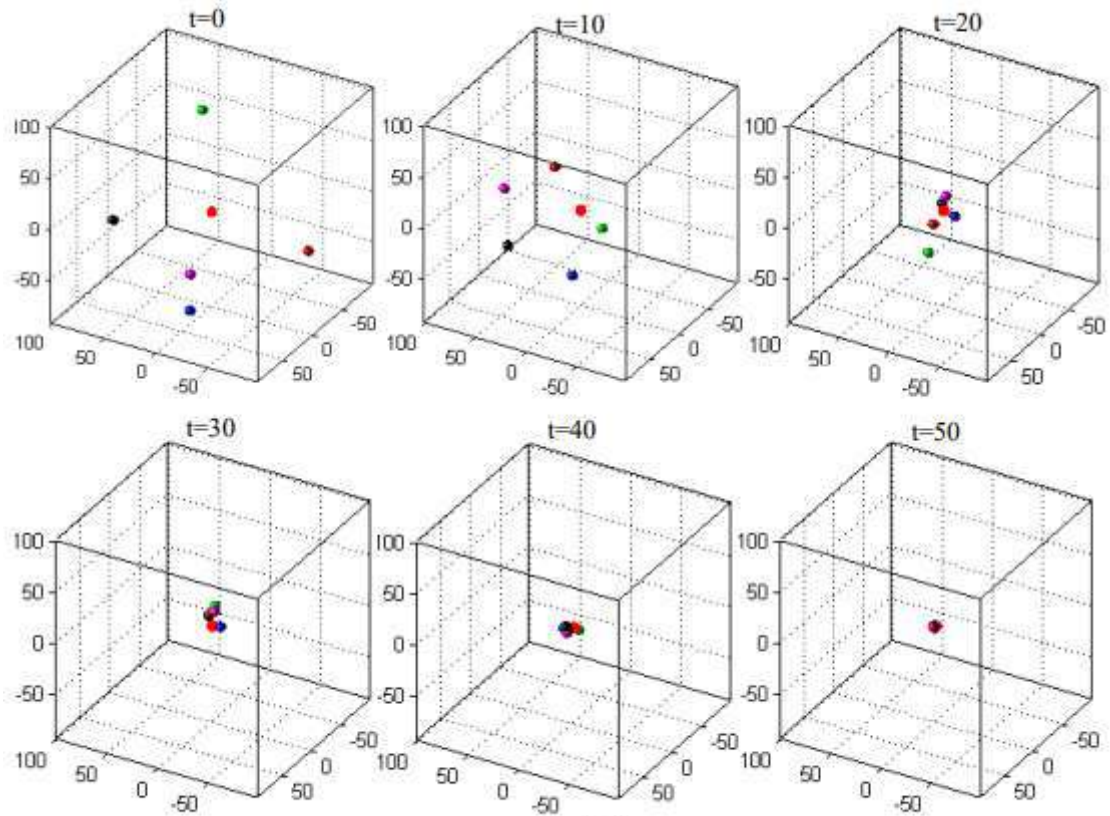


**Fig II.6:** Swarm motion of 5 atoms around a target in a 3-D space.

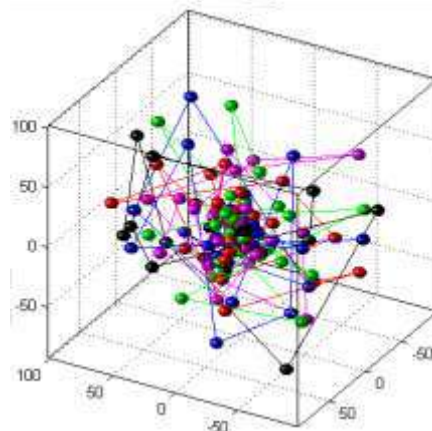


**Fig II.7:** Motion histories of 5 atoms during 50 iterations.

### II.2.5 Framework of ASO algorithm

ASO starts the optimization by generating a set of random solutions. The atoms update their positions and velocities in each iteration, and the position of the best atom found so far is also updated in each iteration. In addition, the acceleration of atoms comes from two parts. One is the interaction force caused by the L-J potential, which actually is the vector sum of the attraction and the repulsion exerted from other atoms. Another is the constraint force caused by the bond-length potential, which is the weighted position difference between each atom and the best atom. All the updating and the calculation are performed interactively until the stop criterion is satisfied. Finally, the position and the fitness value of the best atom are returned as an approximation to the global optimum. The pseudo code of ASO algorithm is provided in figure II.8 [5].

```

Randomly initialize a set of atoms  $X$  (solutions) and their velocity  $v$ , and  $Fit_{Best} = \text{Inf}$ .
While the stop criterion is not satisfied do
  For each atom  $X_i$  do
    Calculate the fitness value  $Fit_i$ ;
    If  $Fit_i < Fit_{Best}$  then
       $Fit_{Best} = Fit_i$ ;
       $X_{Best} = X_i$ ;
    End If.
    Calculate the mass using equations ( II.26) and ( II.27);
    Determine its  $K$  neighbors using equation ( II.32);
    Calculate the in traction force  $F_i$  and the constraint force  $G_i$  using equations ( II.20)
    and ( II.23), respectively;
    Calculate the acceleration using equation ( II.25);
    Update the velocity using equation ( II.30);
    Update the position using equation ( II.31);
  End For.
End While.
Find the best solution so far  $X_{Best}$ 

```

**FigII.8:** Pseudo code of ASO algorithm.

ASO algorithm is very simple to implement and does not require many parameters except for the maximum number of iterations, the number of the atom population, and the dimension of problems to be solved, which are common parameters to all optimization algorithms. Moreover, the upper limit and the starting point of the lower limit can be selected as fixed values by the analysis of figure II.4. In equation (II.18), when the starting point of function '  $F'$  ' is fixed at  $g_0 = 1.1$  , ASO algorithm performs well. The upper limit should be set as:  $u = 1.24$ , which is the maximum value of function  $F'$  . Therefore, the only parameters to be determined are the depth and multiplier weights. Empirically, it is recommended to set them in the range from 0 to 100 and from 0 to 1, respectively. The values of these parameters can be properly selected by four different benchmark functions, namely the Sphere, Rosen

rock, Ackley, and Griewank functions. For each test function, all combinations of the following sets of parameter values are adopted [5].

$$\alpha = [10; 20; 30; 40; 50; 60; 70; 80; 90; 100]$$

$$\beta = [0.1; 0.2; 0.3; 0.4; 0.5; 0.6; 0.7; 0.8; 0.9; 1]$$

Through testing these functions, it can be found that their valley bottom with the optimum can be obtained for parameter ranges of  $40 \leq \alpha \leq 60$  and  $0.1 \leq \beta \leq 0.3$ . Nevertheless, different problems may require a single value for each parameter, so the parameters of ASO are set as  $\alpha = 50$  and  $\beta = 0.2$  in the following experiments [5].

With the above formulation of ASO, the following remarks are made:

(1) ASO inherits the innate stochastic motion of atoms in the real world, hence it intrinsically has the high exploration ability in the search space and thus can well avoid being trapped into the local optima compared to its competitors.

(2) ASO is also a population-based optimization algorithm where the interaction forces include attraction and repulsion. The constraint force is an important media for delivering information within the population.

(3) The attraction and repulsion can guarantee the exploration and exploitation, respectively, with the lapse of iterations. The drift factor can enable the interaction forces exerted on the atoms to gradually witch from the combination of attraction and repulsion to the repulsion alone, thus indicating the switch from the exploration to the exploitation

(4) In the former phase of ASO, whether the interaction forces exerted on the atoms show the attraction or the repulsion depends on the function value of the ratio of  $r_{ij}(t)$  to  $\sigma_i(t)$ , and  $\sigma_i(t)$  can adaptively adjust the category (attraction or repulsion) of the interaction forces acted on the atoms.

(5) The atoms with better fitness values have a larger mass, which leads to a smaller acceleration, thus signifying the local search. Atoms with worse fitness values have the lighter mass, thus signifying the global search.

(6) Each atom in the population interacts only with its neighbors  $KBest$  by the interaction force. The number of  $KBest$  gradually decreases with the lapse of iterations. Meanwhile, each atom and the best one always generate the constraint force at each iteration.

## II.3 Backgrounds

### II.3.1 Structural health monitoring

SHM is a process of implementing damage-identification strategies that is based on the use of robust and reliable indicators that enable the identification, location, quantification and, if possible, damage prediction. In mechanical structures, providing a reliable method that is able to reduce the damage inspection area is crucial for reducing cost and time. These systems mean that scheduled maintenance can be replaced with necessary maintenance so that the structure would have no problem with out-of-date maintenance. This reduces downtime and maintenance costs [6].

The SHM method needs structural signal acquisition and advanced signal processing in order to identify damages. According to [20], the sensors are responsible for detecting, locating and measuring the severity of the structural damage found. Thus, the inclusion of sensors in structural integrity monitoring systems from the design stage is a way to greatly reduce the life-cycle cost. With sensors, monitoring systems can ensure greater safety and reliability in detecting various types of structural damage, reducing maintenance costs [6].

Most methods that use signal processing are based on the relationship between the structural condition and the symptom given by the collected signal. This relationship is not simple, and the complexity found to analyze the most diverse mechanical structures in use today requires the use of advanced systems [6]. According to [6], the inspection of a structure in relation to damage can be divided into five levels: identification, location, evaluation, structural life prediction and intelligent prognosis of the damage. The method used in this work focuses on the second and third items, in which inverse optimization methods will evaluate the damage in terms of its magnitude and severity [6].

### II.3.2 Crack tip formulation in thin plates

A damaged structure will have a different mechanical behavior than a healthy structure. These parameters are directly affected by the variation of the physical properties of the structure, such as its mass and rigidity. In general, structural damage causes a local reduction of the stiffness of the structure and, as a consequence, modifies its characteristics. These modifications become noticeable when analyzing dynamic characteristics of the Lichtenberg optimization algorithm studied model. An example is the difference in vibration modes. Loss of stiffness causes the vibration mode to vary, and in reference to vibration modes of healthy structures, an optimization algorithm can process signals and identify damage [6].

The method of this work is used for crack identification [7] propose a crack model that says that for the crack to propagate in the material, there must be a propagation force acting on the tip of this crack, so that if the force is zero, there is no propagation and the crack is said to be stable. In the context of this work, it is known that there is a crack in the part and its location; however, we want to know about its stability and where it will propagate if it is not stable. FigureII.9 illustrates this model [6].

As long as the force at the crack tip does not exceed the strength limit of the material the frame can still be used, and there is no need to change the material as the crack will not propagate. If the force at the tip of a crack exceeds the maximum strength of the material, it will propagate. Performing corrective structural repair tasks is necessary. These tasks are mainly based on the knowledge of the position (location) and the direction of crack propagation. These parameters can be obtained by the inverse method presented in this work. This way you can only change the affected part of the structure. This is also in agreement with [6], who identified that the crack always arises in the region of maximum principal stress and has its direction [6].

It is important to state that several studies [6] address and present two-dimensional problems owing to their relevance in real structures. In this sense, this study has as hypothesis the study of cracks in plane.

To detect the approximate position of the crack tip, the magnitude of the propagation force at the crack tip, the direction of propagation, remote monitoring of the crack and the forces acting on the crack tips will be performed. Once the force is found to have exceeded the strength limits of the material, it is set aside for removal and replacement. The material is removed in the crack region where the crack is propagating, thus avoiding the exchange of the entire structure [6].

### II.3.3 Lichtenberg algorithm

Optimization can be defined as a process of searching for the best solution within a set of possible solutions. Optimization objectives can be diverse, such as minimizing energy consumption and costs, and maximizing profit, production, performance and efficiency. But real-world optimization problems almost always deal with functions where the analytical solution is impractical because the function may not be continuous, may have no gradient, may be multimodal and not linear and may have many variables and constraints, becoming a very complex problem. To solve them, numerical tools such as meta heuristic optimization algorithms become very important [6].

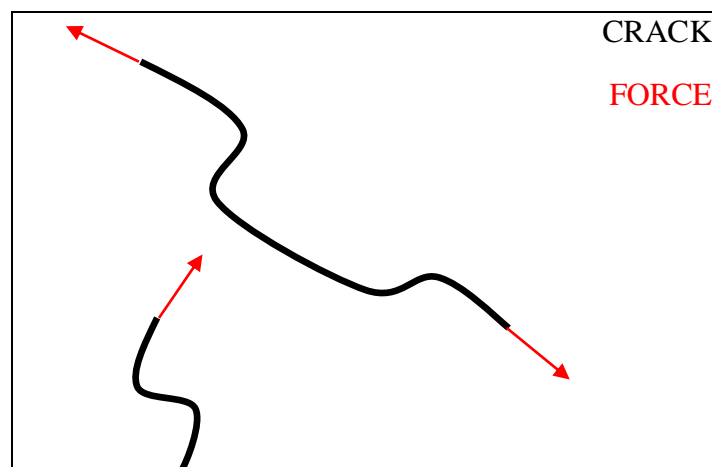


**Fig II.9:** Crack propagation model in thin plates.



The LA is a new hybrid meta heuristic that has trajectory and population algorithm behaviors in its iteration process. Inspired by the physical phenomena of thunderstorms and more precisely radial intra-cloud lightning, where the Lichtenberg figures and the power of fractals can be applied, the LA has great potential for exploring the search space and enhancing solutions already found. It also presented results with excellent precision in test functions found in the literature [6].

The algorithm creates Lichtenberg figures using the diffusion-limited aggregation theory in the search space with random scales and rotations at each iteration. Points of this structure are selected for evaluation of the objective function, and the lowest value point of each iteration is the trigger point of the next figure. Thus, the population is distributed according to the size of the figure, which can reduce or enlarge the search space in approaches of almost 0%–100% of its size, giving the algorithm great exploitability and enhancement of its solutions. Figure II.10 illustrates some iterations of algorithm execution in optimizing two-dimensional functions. Also, this same figure can be plotted with an identical but smaller one (ranging from 0% to 100% of its size) to increase the refinement of the search. Thus, we have local (red) and global (blue) figures [6].

This optimizer has seven parameters:

- (1) figure creation radius ( $R_c$ );
- (2) number of particles used in its construction ( $N_p$ );
- (3) adhesion coefficient ( $S$ ) that determines the density of the cluster;
- (4) local search refinement( $ref$ );
- (5) small print or not to improve result refinement ( $ref$ );
- (6) construction or not of a new Lichtenberg figure at each iteration ( $M$ ), remembering that even if it is the same figure, it is always printed in different rotations;
- (7) scale and the number of iterations ( $N_{iter}$ )

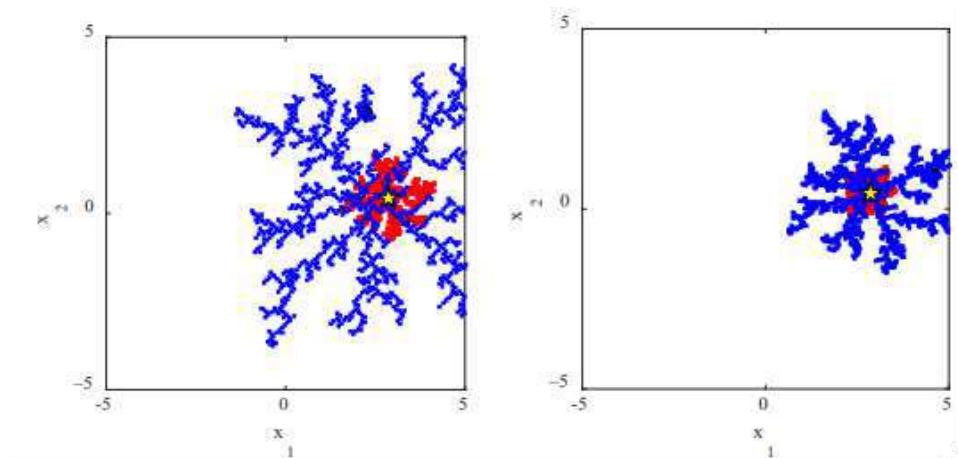


**Fig II.10:** Local figure with 30% of global size figure and some iterations.

## II.4 Mexican Axolotl Variable Optimization

This section explains the proposed bio-inspired optimization procedure.

### II.4.1 The Axolotl in Nature

The axolotl measures a bout 15cm in total length, with it being the specimens that measure more than 30 cm. The axolotl has the appearance of a giant tadpole with legs and a tail. It is characterized by having three pairs of gills, which come out from the base of its head and go backwards, small eyes, smooth skin and legs whose fingers are thin and pointed, but which do not develop nails [8].

In science, the axolotl is known for its extraordinary ability to regenerate amputated limbs and other organs and tissues of the body. It has been observed, for example, that if these animals lose a limb, they are able to regenerate it in a matter of weeks, with all their bones, muscles, and nerves in the appropriate places [8]. Even more fascinating, the researchers say, is the axolotl's ability to repair its spinal cord when it is injured and make it function as if it had not been damaged. It can also repair other tissues such as the retinal tissues and heal wounds without leaving scars. They can also easily accept transplants from other individuals, including the eyes and parts of the brain, restoring their full functionality [8].

### II.4.2 The Artificial Axolotl

The proposed Mexican Axolotl Optimization (MAO) algorithm inspired by the life of the axolotl is explained in this section. We were inspired by the birth, breeding and restoration of the tissues of the axolotls, as well as the way they live in the aquatic environment. As axolotls are sexed creatures, our population is divided into males and females. We also consider the ability of axolotls to alter their color, and we consider they alter their body parts' color to camouflage themselves and avoid predators [8].

Let us assume that we have a numeric optimization problem, defined by a function  $O$  whose arguments are vectors of dimension  $D$ , such that each dimension  $d_i$  is bounded by  $[mini, maxi]$ . We also have a set of solutions (axolotls) of size  $np$ , conforming the population  $P = S_1, \dots, S_{np}$ , and each solution (axolotl)  $S_j \in P, 1 \leq j \leq np$ , is represented as a vector of form  $S_j = s_{j1}, \dots, s_{jD}$ , with  $mini \leq s_{ji} \leq maxi$ , such that  $O$ .

The proposed MAO algorithm operates in four iterative stages, defined by the TIRA acronym: Transition from larvae to adult state, Injury and restoration, Reproduction and Assortment.

First, the initial population of axolotls is initialized randomly. Then, each individual is assigned as male or female, due to axolotls developing according to their sex, and two subpopulations are obtained. Then, the Transition from larvae to adult begins. Male individuals will transition in water, from larvae to adult, by adjusting their body parts' color towards the male who is best adapted to the environment (Figure II.11).



<i>Transitions procedure</i>
Input parameters : Differentiation constant : $\lambda \in [0,1]$ ; Male population: M; Optimisation values for male population: OM; Female population: F; Optimisation values for female population : OF; current number of evaluations $E$
Outputs: Updated male and female population M and F, Updated number of evaluations $E$
Phase 1. Transition from larvae to adult state; $r, r \in [0,1]$ are random numbers 1. Select the best male $m_{best}$ and female $f_{best}$ axolotl, according to the function $O$ 2. For each male axolotl $m_j$ , with optimization value $om_j$ and $1 \leq j \leq  M $ 2.1. Compute the inverse probability of transition, as 2.2. If $pm_j < r$ , then update each component $i$ of the current axolotl as $m_{ji} \leftarrow m_{ji} + (m_{best,i} - m_{ji}) * \lambda$ ; else $m_{ji} \leftarrow min_i + (max_i - min_i) * r_i$ 2.3. Update the optimization value as $om_j \leftarrow O(m_j), E \leftarrow E + 1$ 2.4. Update $m_{best}$ 3. For each female axolotl $f_j$ 3.1. Compute the inverse probability of transition, as $pf_j = \frac{of_j}{\sum of_j}$ 3.2. If $pf_j < r$ , then update each component $i$ of the current axolotl as $f_{ji} \leftarrow f_{ji} + (f_{best} - f_{ji}) * \lambda$ ; else $f_{ji} \leftarrow min_i + (max_i - min_i) * r_i$ 3.3. Update the optimization value as $of_j \leftarrow O(f_j), E \leftarrow E + 1$ 3.4. Update $f_{best}$

**FigII.11:** Pseudo code of the Transition procedure, corresponding to the Transition from larvae to adult state phase in the Mexican Axolotl Optimization (MAO) algorithm.

We assume that best adapted individuals have better camouflage, and the other individuals will change their color accordingly. However, the ability of the axolotls to change color is limited, and we do not want every individual to be able to fully adapt towards the best, which is why we introduce an inverse probability of transition. According to such probability, an axolotl will be selected to camouflage towards the best [8].

Let  $m_{best}$  be the best adapted male (the one with best value of the objective function  $O$ ), and  $\lambda$  be a transition parameter in  $[0,1]$  for the male axolotl  $m_j$ , which will change its body parts' color as in Equation (II.33).

$$m_{ji} \leftarrow m_{ji} + (m_{best,i} - m_{ji}) * \lambda \quad (II.33)$$

Similarly, female axolotls change their bodies from larvae to adults towards the female with best adaptation, using Equation (II.34), where  $f_{best}$  is the best female and  $f_i$  is the current female axolotl.

$$f_{ji} \leftarrow f_{ji} + (f_{best,i} - f_{ji}) * \lambda \quad (II.34)$$

However, and according to the inverse probability of transition, dummy individuals unable to camouflage themselves towards the best and having their own colors are selected. To do so, if a random number  $r \in [0,1]$  is lower than the inverse probability of transition, the corresponding individual is selected. For a minimization problem, for a male axolotl  $m_j$ , with optimization value  $m_j$  the inverse probability of transition is computed as in Equation (II.35); for female axolotl  $f_j$ , with optimization value  $m_j$  we use Equation (II.36). The worst individuals will have greater chances of random transition.

$$pm_j = \frac{om_j}{\sum om_j} \quad (II.35)$$

$$pf_j = \frac{of_j}{\sum of_j} \quad (II.36)$$

Those individuals will transition their  $i$ -th body parts randomly (considering each body part as a function dimension), as in Equations (II.37) and (II.38), where  $r_i \in [0,1]$  is a random number chosen for each  $i$ -th body part. The individuals with random transition will be selected according to the value of the optimization function.

$$m_{ji} \leftarrow min_i + (max_i - min_i) * r_i \quad (II.37)$$

$$f_{ji} \leftarrow min_i + (max_i - min_i) * r_i \quad (II.38)$$

In moving across the water, axolotls can suffer accidents and be hurt. This process is considered in the Injury and restoration phase. For each axolotl  $S_i$  in the population (either male or female), if a probability of damage ( $dp$ ) is fulfilled, the axolotls will lose some part or parts of its body. In the process, using the regeneration probability ( $rp$ ) per bit, the axolotl will lose the  $j$ -th body part (bit), and will replace it as

$$p'_{ji} \leftarrow min_i + (max_i - min_i) * r_i \quad (II.39)$$

Where:

$0 \leq r_i \leq 1$  is randomly chosen for each body part.

The pseudo code of the Injury and Restoration phase of the Mexican Axolotl optimization algorithm is provided in figure II.12. Then, the Reproduction of the population begins. The pseudo code of the Reproduction and Assorting phase is given in Figure II.13. For each female axolotl in the population, a male is selected from which offspring will be obtained. To do so, we use to uniment selection [8].

<i>Accidents</i> procedure
Input parameters: Male population : M; Optimization values for male population: OM; Female population: F; Optimization values for female population: OF; current number of evaluations E, Damage probability: $\lambda \in [0,1]$ ;Regeneration probability: $rp \in [0,1]$ ;
Outputs : Updated populations M and F, updated number of evaluations $E$
Phase 2. Injury and restoration; $r, r_i \in [0,1]$ are random numbers 1.For each male axolotl $m_j$ 1.1. If $r \leq dp$ 1.1.1. For $i=1 \dots D$ 1.1.1.1. If $r \leq dp$ then $m_{ji} \leftarrow \min_i + (\max_i - \min_i) * r_i$ 1.1.2. $om_j \leftarrow \mathbf{O}(m_j), E \leftarrow E + 1$ 1.2. Update $m_{best}$ 2. For each female axolotl $f_j$ 2.1. If $r \leq dp$ 2.1.1. For $i=1 \dots D$ 2.1.1.1. If $r \leq dp$ then $f_{ji} \leftarrow \min_i + (\max_i - \min_i) * r_i$ 2.1.2. $of_j \leftarrow \mathbf{O}(f_j), e \leftarrow e + 1$ 2.2. Update $f_{best}$

**FigII.12:** Pseudo code of the Accidents procedure, corresponding to the Injury and restoration state phase in the MAO algorithm.

After that, the male places spermatophores and the female collects them with the cloaca to deposit them in her sperma theca. The eggs are formed using the genetic information of both parents uniformly (figure II.14). For simplicity, we assume that each pair of male and female axolotls has two eggs. The female deposits the eggs and waits until hatching. Once hatching, the Assortment process starts. The newly created individuals (larval state) will compete with their parents to be in the population. If the young are better according to the objective function, the young will replace them [8].

<i>New Life</i> procedure
<p>Input parameters:  Tournament size: <math>k \in [1, np]</math>; Male population: <math>M</math>; Optimization values for male population: <math>OM</math>; Female population: <math>F</math>; Optimization values for female population: <math>OF</math>; current number of evaluations <math>E</math></p>
<p>Outputs:  Updated male and female populations <math>M</math> and <math>F</math>,  Updated number of evaluations <math>E</math></p>
<p>Phase 3. Reproduction and Assortment ; <math>r_i \in [0,1]</math> is a random number  1. For each female axolotl <math>f_j</math>  1.1. Select a suitable male <math>m_j \in M</math>, using tournament selection of size <math>k</math>  1.2. Option two eggs, <math>egg_1</math> and <math>egg_2</math> by uniformly combining the body parts of the parents, as follows:  1.2.1. For <math>i=1 \dots D</math>  1.2.1.1. If <math>r_i \leq 0.5</math>, then <math>egg_{1i} \leftarrow m_{ji}</math> and <math>egg_{2i} \leftarrow f_{ji}</math>; else <math>egg_{2i} \leftarrow m_{ji}</math> and <math>egg_{1i} \leftarrow f_{ji}</math>  1.3. Compute the fitness of the eggs, as <math>oegg_1 \leftarrow O(egg_1)</math> and <math>oegg_2 \leftarrow O(egg_2)</math>, <math>E \leftarrow E + 2</math>  1.4. Sort <math>f_j, m_j, egg_1, egg_2</math> according to their optimisation values.  1.5. Assign the first individual in the ranking to <math>f_j</math>, and the second-best to <math>m_j</math></p>

**FigII.13:** Pseudo-code of the New Life procedure, corresponding to the Reproduction and Assortment phase in the MAO algorithm of the proposed Mexican Axolotl Optimization.

$m_{parent} = [0.32, 4.56, 6.08, 0.54, 1.67]$ $f_{parent} = [1.23, 5.43, 7.83, 0.76, 4.34]$ Offspring: $rdm = [0.1, 0.3, 0.7, 0.3, 0.9]$ $off\_1 = [1.23, 5.43, 6.08, 0.76, 1.67]$ $off\_2 = [0.32, 4.56, 7.83, 0.54, 4.34]$
---

**FigII.14:** Reproduction in the MAO. (a) Male parent, (b) female parent, (c) random numbers generated to uniformly distribute the parents' information, and (d) the resulting offspring.

After the Assortment procedure, the TIRA process (Phase 1. Transition from larvae to adult state; Phase 2. Injury and restoration and Phase 3. Reproduction and Assortment) repeats, until the stopping condition of the algorithm is fulfilled. Figure II.15 shows the pseudo code of the proposed MAO algorithm, considering a minimization problem.

The proposed Mexican Axolotl Optimization algorithm incorporates in the optimization process several aspects of the life of the axolotl, such as its aquatic development, its ability to transform its body from larvae to adult state, its sexed reproduction, and its capability of regenerating organs and body parts [8].

Our proposal differentiates from other evolutionary and swarm intelligence algorithms in the following:

1. We divide the individuals into males and females.
2. We consider the females more important, due to the fact that for each female we find the best male according to tournament selection, to obtain the offspring.
3. We have an elitist replacement procedure to include new individuals in the population. In such a procedure, the best individual is considered to be a female, and the second-best to be a male. That is, our procedure has the possibility of converting a male into a female, if the male is best.

In the following, we address the experiments made to evaluate MOA for numerical optimization [8].

<i>Mexican Axolotl Optimization</i>
Input parameter: Population : P; P size: np, Female population: F; Male population :M; Damage probability   Regeneration probability: $dp \in [0,1]$ ; Regeneration probability: $rp \in [0,1]$ ; Differentiation constant : $\lambda \in [0,1]$ ; Tournament size: $k \in [0, np]$ ; Termination criteria: number of evaluations (eval) Of objective function $O$ ; Number of dimensions of the function: D; Limits of the variables: $[min_i, max_i]$ , with $i \in \{1, \dots, D\}$
Output : Best axolotl ( $b\_axolotl$ )
Initialization 1. Obtain a random population of size np and evaluate it according to $O$ <ol style="list-style-type: none"> <li>1.1. <math>P = \emptyset, OM = \emptyset, OF = \emptyset, E = 0</math></li> <li>1.2. For <math>j = 1..np</math> <ol style="list-style-type: none"> <li>1.2.1. Create an axolotl <math>p_j</math> as a vector of size D, with random components in the limits of the variables</li> <li>1.2.2. <math>P \leftarrow O(p_j), E \leftarrow E + 1</math></li> <li>1.2.3. <math>P \leftarrow P \cup \{p_j\}, OP \leftarrow OP \cup \{op_j\}</math></li> </ol> </li> </ol> 2. Divide the population in males and females <ol style="list-style-type: none"> <li>2.1. <math>M = \emptyset, F = \emptyset</math></li> <li>2.2. For <math>j = 1..np</math> <ol style="list-style-type: none"> <li>2.2.1. If <math>i</math> is an odd number               <ol style="list-style-type: none"> <li>2.2.1.1. <math>M \leftarrow M \cup p_j,</math></li> <li>2.2.1.2. <math>om_j \leftarrow O(p_j), E \leftarrow E + 1</math></li> <li>2.2.1.3. <math>OM \leftarrow OM \cup om_j,</math></li> </ol> </li> <li>2.2.2. else               <ol style="list-style-type: none"> <li>2.2.2.1. <math>F \leftarrow F \cup \{p_j\}</math></li> <li>2.2.2.2. <math>of_j \leftarrow o(p_j), E \leftarrow E + 1</math></li> <li>2.2.2.3. <math>OF \leftarrow OF \cup of_j,</math></li> </ol> </li> </ol> </li> </ol> Iterative phases 3. While $E \leq eval$ <ol style="list-style-type: none"> <li>3.1. <math>\{\lambda, M, OM, F, OF, E\} \rightarrow</math> Transition <math>\rightarrow \{M', OM', F', OF', E'\}</math> // Phase 1</li> <li>3.2. <math>\{dp, rp, M', OM', F', OF', E'\} \rightarrow</math> Accidents <math>\rightarrow \{M'', OM'', F'', OF'', E''\}</math> // Phase 2</li> <li>3.3. <math>\{k, M, OM, F, OF, E\} \rightarrow</math> NewLife <math>\rightarrow \{M''', OM''', F''', OF''', E'''\}</math> // Phase 3</li> <li>4. If <math>o(m_{best}) &lt; O(f_{best})</math> then <math>b\_axolotl \leftarrow m_{best}</math>              Else <math>b\_axolotl \leftarrow f_{best}</math></li> </ol>

**Fig II.15:**Pseudo-code of the proposed Mexican Axolotl Optimization.

## II.5 Equilibrium optimizer

This section presents the inspiration, mathematical model, and algorithm of the Equilibrium Optimizer (EO) [9].

### II.5.1 Inspiration

The inspiration for the EO approach is a simple well-mixed dynamic mass balance on a control volume, in which a mass balance equation is used to describe the concentration of a nonreactive constituent in a control volume as a function of its various source and sink mechanisms. The mass balance equation provides the underlying physics for the conservation of mass entering, leaving, and generated in a control volume. A first-order ordinary differential equation expressing the generic mass-balance equation [9], in which the change in mass in time is equal to the amount of mass that enters the system plus the amount being generated inside minus the amount that leaves the system, is described as:

$$V \frac{dC}{dt} = QC_{eq} - QC + G \quad (\text{II.40})$$

$C$  is the concentration inside the control volume ( $V$ ),  $V dC$  is the rate of change of mass in the control volume,  $Q$  is the volumetric flow rate into and out of the control volume,  $C_{eq}$  represents the concentration at an equilibrium state in which there is no generation inside the control volume, and  $G$  is the mass generation rate inside the control volume. When  $V dC$  reaches to zero, a steady equilibrium state is reached. A rearrangement of equation (II.41) allows to solve for  $dC$  as a function of  $Q V$ ; where  $Q V$  represents the inverse of the residence time, referred to here as  $\lambda$ , or the turnover rate [9].

(i.e.,  $\lambda = Q V$ ). Subsequently, equation (II.40) can also be rearranged to solve for the concentration in the control volume ( $C$ ) as a function of time ( $t$ )

$$\frac{dC}{\lambda C_{eq} - \lambda C + \frac{G}{V}} = dt \quad (\text{II.41})$$

Equation (II.42) shows the integration of equation (II.41) over time

$$\int_{C_0}^C \frac{dC}{\lambda C_{eq} - \lambda C + \frac{G}{V}} = \int_{t_0}^t dt \quad (\text{II.42})$$

This Results in

$$C = C_{eq} + (C_0 - C_{eq})F + \frac{G}{\lambda V} (1 - F) \quad (\text{II.43})$$

In the equation (II.43),  $F$  is calculated as follows

$$F = \exp [-\lambda (t - t_0)] \quad (\text{II.44})$$

Where:

$t_0$  and  $C_0$  are the initial start time and concentration, dependent on the integration interval. Equation (II.43) can be used to either estimate the concentration in the control volume with a known turnover rate or to calculate the average turnover rate using a simple linear regression with a known generation rate and other conditions [9].

EO is designed in this sub-section using the above equations as the overall framework. In EO, a particle is analogous to a solution and a concentration is analogous to a particle's position in the PSO algorithm. As equation (II.43) shows, there are three terms presenting the updating rules for a particle, and each particle updates its concentration via three separate terms. The first term is the equilibrium concentration, defined as one of the best-so-far solutions randomly selected from a pool, called the equilibrium pool. The second term is associated with a concentration difference between a particle and the equilibrium state, which acts as a direct search mechanism. This term encourages particles to globally search the domain, acting as explorers. The third term is associated with the generation rate, which mostly plays the role of an exploiter, or solution refiner, particularly with small steps, although it sometimes contributes as an explorer as well. Each term and the way they affect the search pattern is defined in the following [9].

## II.6 Conclusion

In this chapter we reviewed the real-life optimization problems. And it involves different types of constraints. The classical derivative-based optimization techniques often fail to solve such type of problems. These difficulties motivate us to develop alternative and effective ways to solve them.

We discussed to atom search optimization (ASO), numerous bio-inspired algorithms had been proposed for numerical optimization and Lichtenberg algorithm (LA) and Mexican Axolotl Variable Optimization and Equilibrium optimizer, we also discussed to equilibrium optimizer.



**Chapter III**  
**Simulations and Results**



### III.1 Introduction

Those typical test cases includes four units which are one conventional power unit, one heat unit and three cogeneration CHP units. The test cases power demand is 300MW and the test case heat demand is 150MWth. Based on references [10], the specific model parameters used in this test case are described in detail as follows:

- ✓ The cost and emission function of each unit of test system 2 Power-Only units are given:

$$C_{p1}(P_1) = 0.000115P_1^3 + 7.699P_1 + 254.8863\$; \leq P_1 \leq 135MW \quad (III.1)$$

$$E_{p1}(P_1) = 10^{-4} \times (6.490P_1^2 - 5.554P_1 + 4.091) + 2 \times 10^{-4} \times \exp(0.02857P_1)Kg \quad (III.2)$$

The fuel cost and emission formulations of the CHP units are given:

$$C_{c1}(O_1; H_1) = 0.04535O_1^2 + 36O_1 + 1250 + 0.027H_1^2 + 0.6H_1 + 0.011O_1H_1\$ \quad (III.3)$$

$$E_{c1}(O_1; H_1) = 0.00165O_1Kg \quad (III.4)$$

$$C_{c2}(O_2; H_2) = 0.1035O_2^2 + 34.5O_2 + 2650 + 0.025H_2^2 + 2.203H_2 + 0.051O_2H_2\$ \quad (III.5)$$

$$E_{c2}(O_2; H_2) = 0.0022O_2Kg \quad (III.6)$$

$$C_{c3}(O_3; H_3) = 0.072O_3^2 + 20O_3 + 1565 + 0.02H_3^2 + 2.3H_3 + 0.04O_3H_3\$ \quad (III.7)$$

$$E_{c3}(O_3; H_3) = 0.0011O_3Kg \quad (III.8)$$

- ✓ **Feasible Operation Region of the CHP Units**

The feasible operation region (FOR) of the CHP unit 2 of the test system2 is provided in figure III.1 and the inequality constraints for this unit is provided by (III.9).

$$\begin{aligned} \frac{15}{55}H_2 + O_2 - 60 \leq 0; \frac{35}{15}H_2 - O_2 - \frac{1250}{15} \leq 0 \\ -\frac{10}{40}H_2 - O_2 + 20 \leq 0 \end{aligned} \quad (III.9)$$

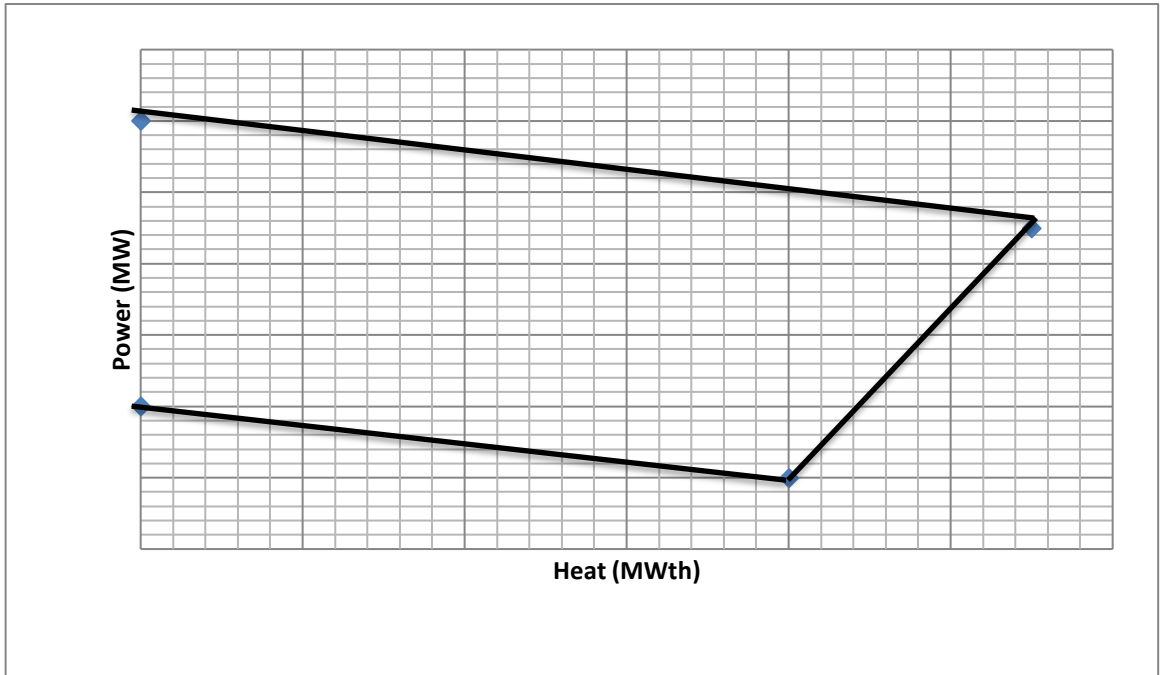


**Fig III.1:** Heat-power feasible operating region for the CHP unit 2 of test system 2.

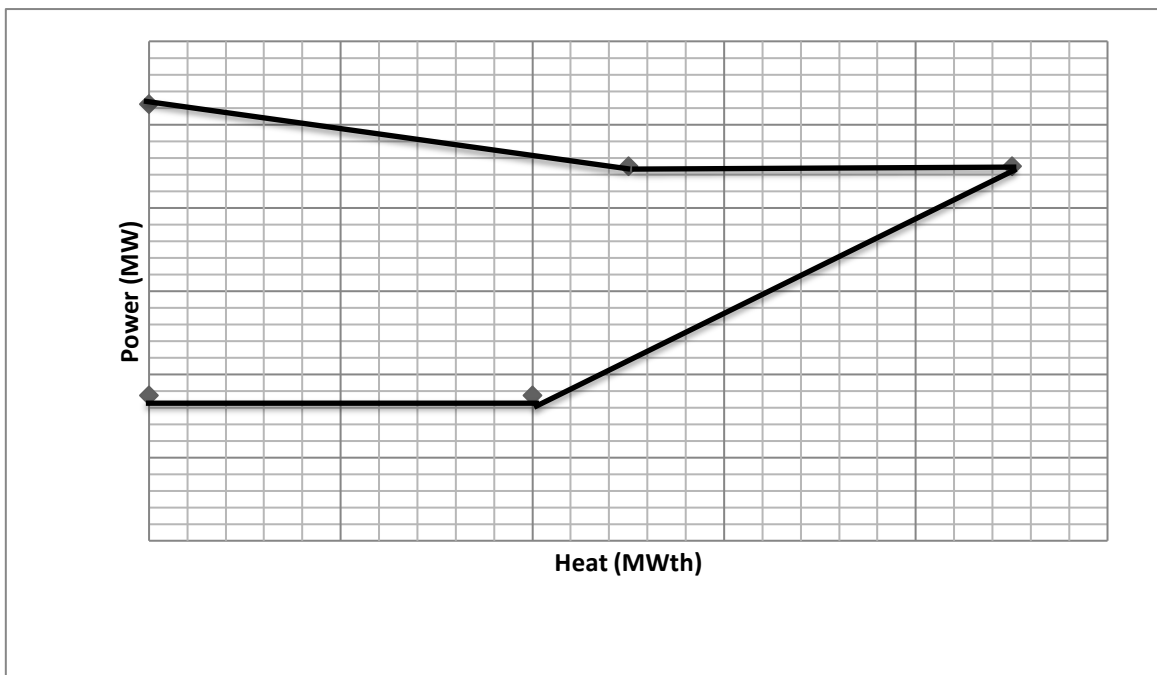


**Fig III.2:** Heat-power feasible operating region for the CHP unit 3 of test system 2.

The FOR of the CHP unit 3 of the test system 2 is shown in Figure III.2 and the inequality constraints for this unit is given by (III.10) and (III.11).

$$O_3 = 90 \Rightarrow 25 \leq H_3 \leq 45;$$

$$O_2 = 35 \Rightarrow 0 \leq H_2 \leq 20; \quad (III.10)$$

$$\frac{15}{25}H_3 + O_3 - 105 \leq 0; \frac{55}{25}H_3 - O_3 - 9 \leq 0 \quad (III.10)$$

#### ✓ Heat Only Units

$$C_{h1}(T_1) = 0.038OT_1^2 + 2.0109T_1 + 950\$;$$

$$0 \leq T_1 \leq 60 \text{ MWth} \quad (III.11)$$

$$E_{h1}(T_1) = 0.0017T_1 \text{ Kg} \quad (III.12)$$

### III.2 Case 1:

In arriving at the results of optimum as shown in Table I, The meta heuristic techniques such as PSO, IPSO, MPSO, TACPSO, LA, MAO, EO and ASO are employed by the minimization only the fuel cost or the economic dispatch, where the optimal solution is compared with respect to those illustrated by various optimization techniques.

The parameters of algorithms are:

#### LA:

Pop= 400, Niter=500, Np= 1,000,000, S= 0.5, Rc =250, ref= 0.2, M=0.

#### MAO:

Total population size: 30; damage probability  $dp = 0.5$ ; regeneration probability  $rp = 0.1$ ; tournament size  $k = 3$ ; differentiation constant  $\lambda = 0.5$ ; Niter=500.

#### ASO:

Depth weight: 50; Multiplier weight 0.2; Niter=500.

#### EO:

EO uses 30 particles along with 500 iterations;  $a1=2$ ;  $a2 = 1$  and Generation probability  $GP = 0.5$ .

#### PSO:

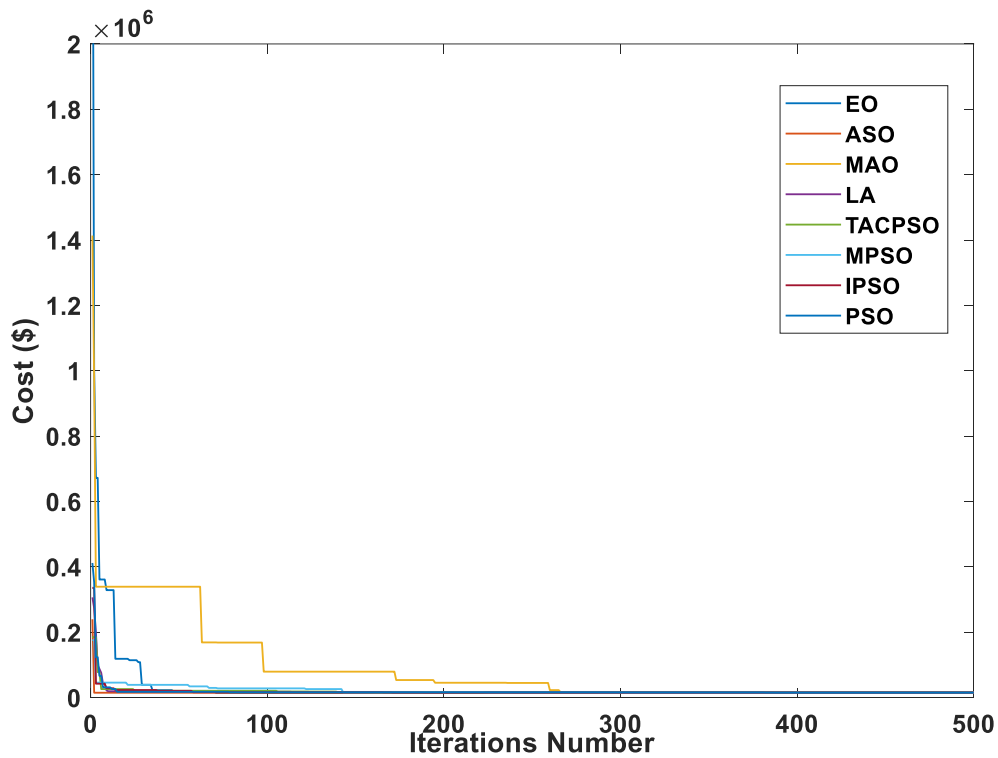
Cognitive constant: 2; Social constant: 2; Inertia constant 0.8; Niter=500.

Items	PSO	IPSO	MPSO	TACPSO	LA	MAO	EO	ASO
P1 MW	100.9382	135.0000	125.4155	81.9876	35.0000	109.3753	135.0000	119.7725
P2 MW	61.9783	108.0107	72.1287	100.2221	119.3782	88.9939	0.0000	95.4554
P3 MW	59.2824	39.5179	59.3185	31.4058	48.0334	28.1275	60.0000	40.2736
P4 MW	77.8012	17.4714	43.1373	86.3845	97.5937	73.5075	104.9990	44.4985
H1MWth	54.4593	55.7605	50.5436	35.9140	50.4350	57.7243	107.2565	69.1740
H2MWth	51.2840	55.0000	55.0000	9.5114	37.1712	25.7424	0.0000	12.4308
H3MWth	16.3044	39.2395	0.0000	44.5746	7.1648	30.9029	0.0000	30.6962
H4MWth	27.9523	0.0000	44.4564	60.0000	55.2261	35.5309	42.7430	37.6991
Cost\$/h	14174,90915	13867,81996	13687,26287	13842,71026	13930,47154	14744,33027	14810,89864	13812,48439
Std\$/h	597.8014	815.5446	959.5857	583.6456	817.2169	950.5760	878.8006	18.0937
Min\$/h	14174.9091	13867.8200	13687.2629	13842.7103	13930.4715	14744.3303	13812.4844	14810.8986
Max\$/h	16629.0589	17162.7300	17108.9790	16243.9801	17124.5680	19329.9695	16998.0111	14878.5976
Mean\$/h	15160.9414	15233.7207	15103.4497	14996.5282	15284.6206	16076.7719	14940.7635	14846.7198
Time S	2.7344	3.8750	3.8750	3.8438	704.0156	950.5760	19.5894	575.2480

TABLE III.1: Simulation results of fuel cost.

Items	PSO	IPSO	MPSO	TACPSO	LA	MAO	EO	ASO
Cost \$/h	14174,90915	13867,81996	13687,26287	13842,71026	13930,47154	14744,33027	14810,89864	13812,48439
Items	BCS 1 [11 ]	BCS 2 [11 ]	NSGA-II [12]	SPEA 2 [12]				
Cost \$/h	14504.2	15137.3	15008.7	14964.3				

TABLE III.2: Comparison results of fuel cost.



FigIII.3: Convergence Curve of Costs.

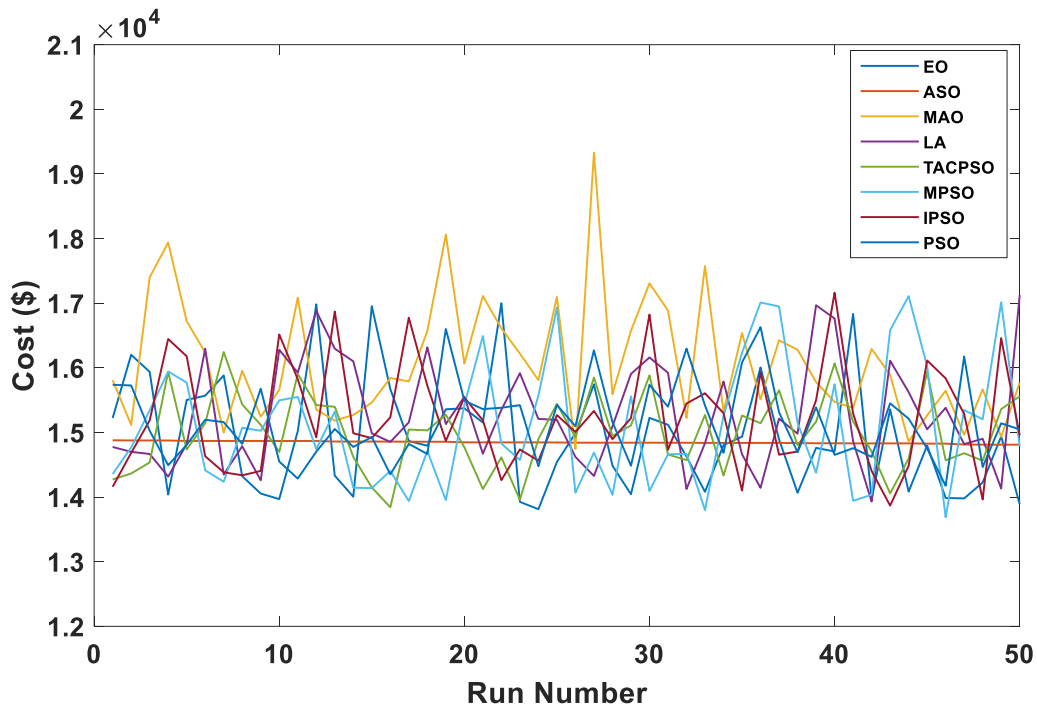


**Fig III.4:** Run Number of Costs.

From Table III.1 Table III.2 and it can be observed that the optimal cost results of different algorithms are different from each other. Compared MPSO, PSO, IPSO, TACPSO, LA, MAO, EO and ASO with the BCSs of NSGA-II and SPEA 2, the cost of MPSO is respectively decreased by 487.64628\$/h, 180.55709, 155.44739, 243.20867, 1057.0674, 1123.63577, 125.22152, 816.93713, 1450.03713, 1321.43713 and 1277.03713\$/h.

Other remark, the constraints equalities are verified, that the summation of powers and heats generated is the same of demand, so equal 300 MW and 150 MWth.

Figure III.1 also shows that all the algorithms propose can produce well spread and diverse solutions. Figure III.2 displays the obtained values (best, average, and max values) among 50 runs of all algorithms technique for the case of minimizing the fuel cost of production.

### III.3 Case 2:

For this case, PSO, IPSO, MPSO, TACPSO, LA, MAO, EO and ASO are implemented for solving only the emission dispatch and the optimal solution is compared with respect to those illustrated by various optimization techniques as manifested in Table III.2.

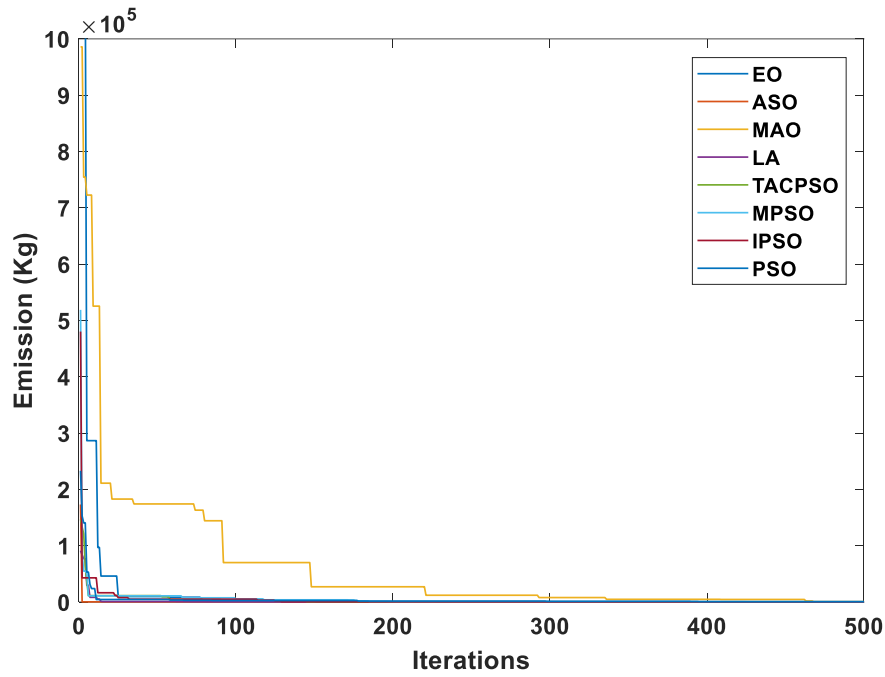
Items	PSO	IPSO	MPSO	TACPSO	LA	MAO	EO	ASO
P1 MW	102.3163	109.9767	135.0000	69.9347	39.5704	107.6459	35.0267	65.0889
P2 MW	75.9826	64.6144	42.6104	93.1036	125.8000	93.0202	125.3476	101.3677
P3 MW	24.6164	52.3193	51.0093	34.8281	50.3200	29.7030	59.5620	52.7216
P4 MW	97.0757	73.0896	71.3803	102.1336	84.3116	69.5975	80.0637	80.8219
H1MWth	110.0632	47.8200	83.0649	58.3171	89.6174	52.9281	97.4530	80.1184
H2MWth	12.1026	14.3020	21.9351	4.8156	23.2515	31.9059	52.5469	35.2996
H3MWth	17.4118	36.6127	45.0000	45.0000	14.8717	16.6057	0.0000	16.5887
H4MWth	10.3832	51.2653	0.0000	41.8674	22.2616	48.5649	0.0000	17.9933
Emis Kg/h	709.7620	371.1671	507.7902	379.3684	265.4392	688.3176	352.6131	328.6705
Std\$/h	158.6150	127.9518	188.7317	108.8027	136.2812	456.1249	131.9613	6.7892
Min\$/h	72.6956	72.7335	46.1791	156.8829	188.2709	349.0494	66.9636	328.6705
Max\$/h	803.1613	815.9668	737.9168	608.0923	741.6044	2344.0234	550.9436	347.8254
Mean\$/h	384.3667	324.3837	328.7567	342.0974	476.1797	1051.2971	272.9817	338.7892
Time S	4.6406	3.8906	3.8750	3.9844	524.1406	456.1249	19.7071	564.0020

TABLE III.3: Simulation results of fuel emission

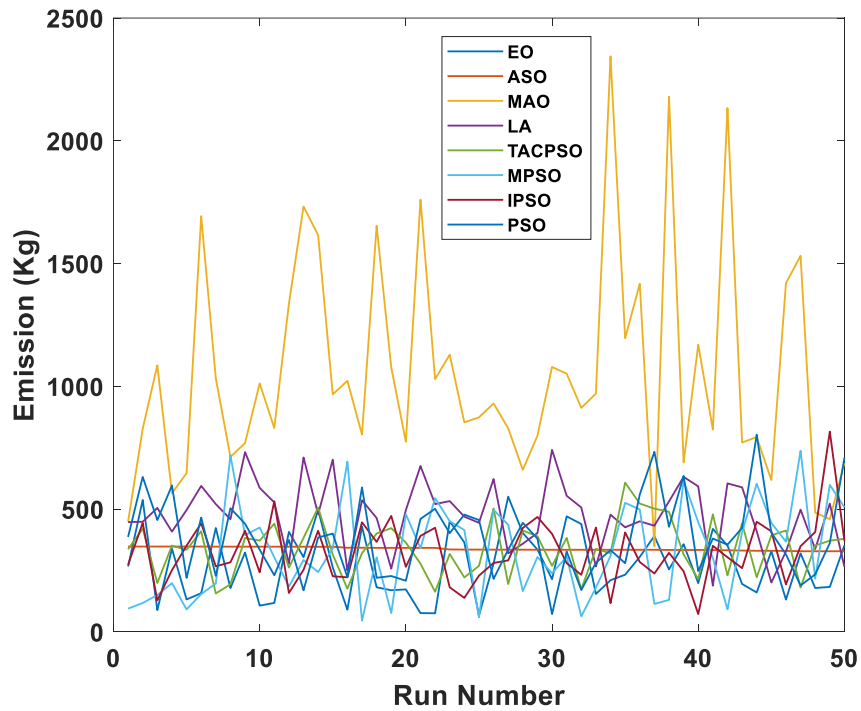
Items	PSO	IPSO	MPSO	TACPSO	LA	MAO	EO	ASO
Emission Kg/h	709,762	571,1671	507,7902	679,3684	765,4392	788,3176	752,6131	728,6705
Items	BCS 1 [11 ]	BCS 2 [11 ]	NSGA-II [12]	SPEA 2 [12]				
Emission Kg/h	750	510	610	640				

TABLE III.4: Comparison results of fuel emission.

From Table III.3 Table III.4 and it can be observed that the optimal results of different algorithms are different from each other. Compared MPSO, PSO, IPSO, TACPSO, LA, MAO, EO and ASO with the BCSs of NSGA-II and SPEA 2, the emission is increased by 201.9718 kg/h, 63.3769 kg/h, 171.5782 kg, 257.649 kg/h, 280.5274 kg/h, 244.8229 kg, 220.8803 kg/h, 242.2098 kg/h, 2.2098 kg/h ,102.2098 and 132.2098kg/h, regarding MPSO respectively.



**FigIII.5:** Convergence Curve of Emissions.



**Fig III.6:** Run Number of Emissions.

Other remark, the constraints equalities are verified, that the summation of powers and heats generated is the same of demand, so equal 300 MW and 150 MWth.

Figure III.3 also shows that all the algorithms propose can produce well spread and diverse solutions. Figure III.4 displays the obtained values (best, average, and max values) among 50 runs of all algorithms technique for the case of minimizing the fuel emission of production.

### III.4 Case 3:

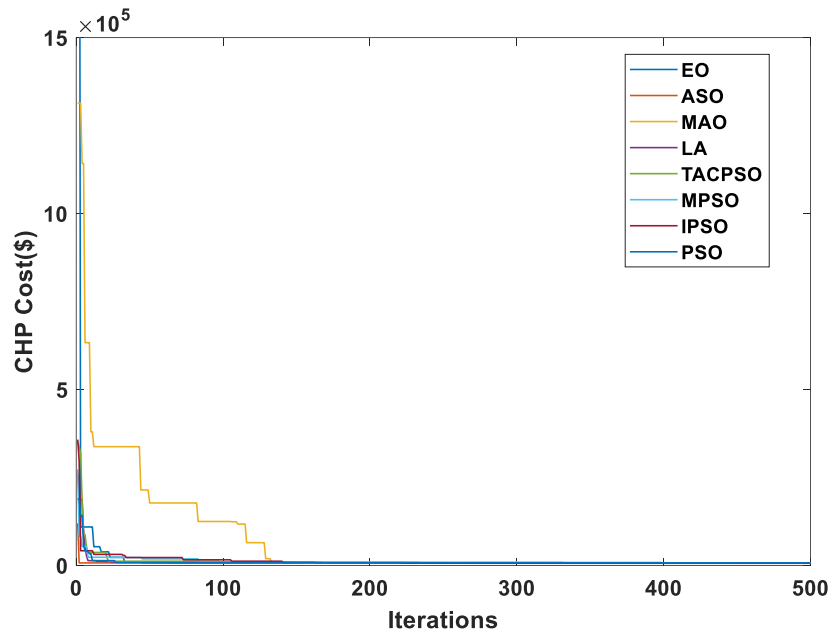
Only the CHP are implemented in this case using PSO, IPSO, MPSO, TACPSO, LA, MAO, EO and ASO for solving the optimal solution and compared with respect to those illustrated by various optimization techniques as manifested in Table III.5.

	PSO	IPSO	MPSO	TACPSO	LA	MAO	EO	ASO
P1 MW	83.1419	130.7181	55.9654	113.9602	110.2851	111.7465	105.9161	74.4061
P2 MW	121.9660	71.2168	125.8000	82.5783	84.9495	98.9616	89.6891	112.1966
P3 MW	37.9238	59.9175	50.7304	25.1932	53.4958	28.3223	0.0321	23.8927
P4 MW	56.9643	38.1476	67.5043	78.2683	51.2847	60.9508	104.3625	89.5046
H1MWth	106.0020	68.8375	83.4021	37.6693	89.8498	52.1887	72.4679	59.1962
H2MWth	10.2979	3.8353	5.9283	43.0225	44.9798	21.2488	34.6930	35.5307
H3MWth	12.5612	42.4917	0.6696	31.8126	12.4331	31.3732	42.8390	32.5092
H4MWth	21.1390	34.8354	60.0000	37.4956	2.7514	45.2140	0.0000	22.7640
Cost\$/h	7066.4447	6108.8924	7397.9391	6274.9119	6895.7423	6772.4618	6507.2941	7118.1539
Std\$/h	416.6126	549.1443	767.8317	527.3443	559.9545	575.5244	548.2004	14.7013
Min\$/h	5844.4321	5550.0016	5567.6700	5624.2842	5997.3875	6369.4797	5600.6195	7118.1539
Max\$/h	7856.4938	7995.3604	8089.1002	7876.6647	7949.2031	9054.0204	7895.3379	7167.2521
Mean\$/h	6728.7040	6521.9020	6725.1713	6583.0527	6875.8432	7231.5924	6391.9990	7140.8742
Time S	4.0938	5.1250	3.8906	4.5938	520.1406	575.5244	38.0343	644.3600

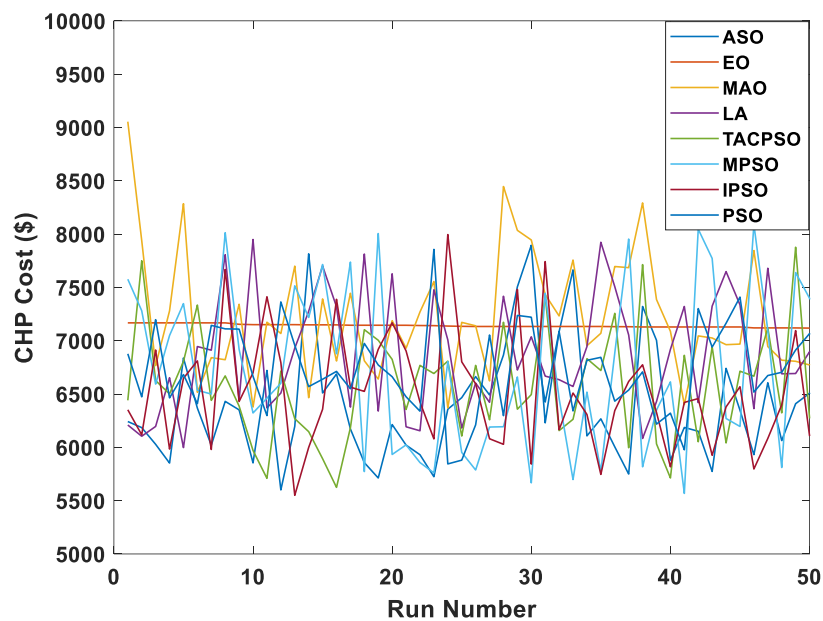
TABLE III.5: Simulation results of CHP fuel cost.

From Table III.5, it can be observed that the IPSO algorithm obtains less CHP cost than the algorithm reported in the existing Table III.5. Other remark, the power production and the heat production are 300 MW and 150 MWth respectively. Transparently, the output result completely fulfills the heat and power demands.





**FigIII.7:** Convergence Curve of CHP Costs.



**FigIII.8:** Run Number of CHP Costs.

Figure III.5 also shows that all the algorithms propose can produce well spread and diverse solutions. Figure III.6 displays the obtained values (best, average, and max values) among 50 runs of all algorithms technique for the case of minimizing the fuel emission of production.

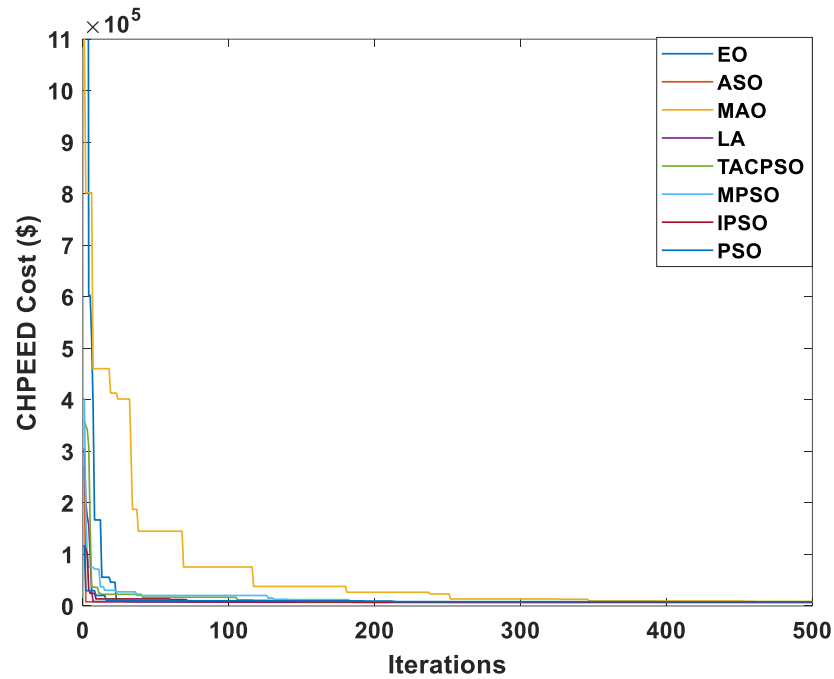
**III.5 Case 4:**

The cost emission combined heat power dispatch (CHPEED) are implemented in this case using PSO, IPSO, MPSO, TACPSO, LA, MAO, EO and ASO for solving the optimal solution and compared with respect to those illustrated by various optimization techniques as manifested in Table III.6.

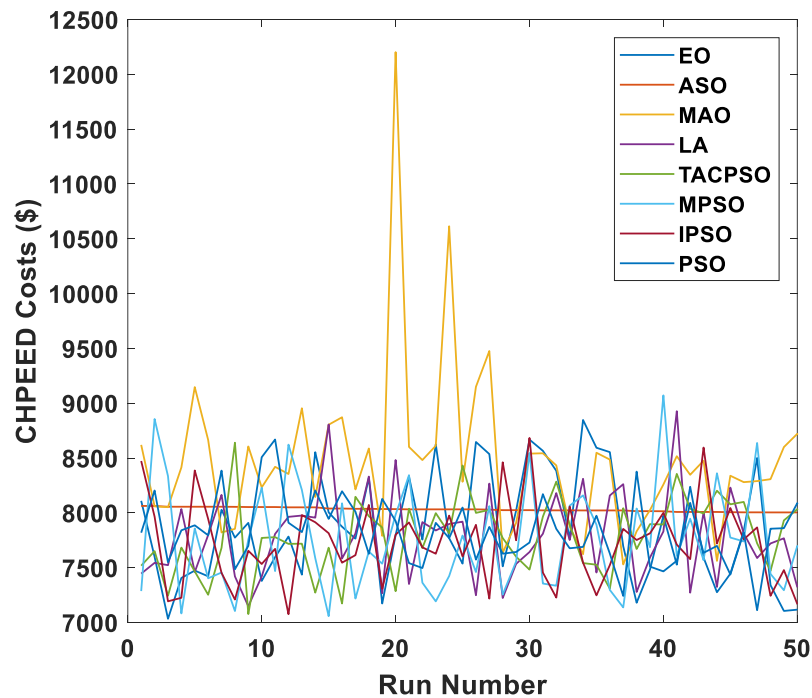
	PSO	IPSO	MPSO	TACPSO	LA	MAO	EO	ASO
P1	72.2060	132.0674	135.0000	79.3289	135.0000	97.4158	134.9994	90.5596
P2	111.3305	68.9084	109.4960	118.7544	78.1680	99.7602	75.5618	110.9192
P3	42.8803	7.9060	49.7412	15.7602	28.4992	48.7322	0.0005	46.9427
P4	73.5832	91.1182	5.7627	86.1565	58.3321	54.0360	89.4373	51.5785
H1	66.1298	85.8853	45.2734	20.8065	97.8006	83.4116	135.5887	83.5868
H2	21.0731	36.5085	0.0031	55.0000	16.0760	13.9177	13.1308	34.5525
H3	13.3857	21.2438	45.0000	14.1935	11.2035	29.2311	0.0051	13.0082
H4	49.4116	6.3624	59.7235	60.0000	24.9310	23.4720	1.2713	18.8524
Cost	8088.7564	7169.3466	7698.1059	8033.6714	7324.1657	8721.2543	7117.3067	8004.2930
Std	310.7987	380.7113	489.8053	337.8620	406.6269	751.2328	493.8197	18.1442
Min	7112.4554	7075.8725	7057.9199	7076.9691	7148.5377	7529.7052	7034.2406	8004.2930
Max	8669.2676	8683.6987	9071.7803	7787.8514	8927.3883	12202.5503	8847.5341	8063.3338
Mean	7831.7173	7725.8701	7758.0365	8639.8552	7787.8753	8474.4140	7857.3031	8031.2336
Temp	3.8594	5.1094	5.1406	5.3750	525.2813	751.2328	20.1324	549.2350

**TABLE III.6:** Simulation results of CHPEED.

The optimal solution is compared with respect to those illustrated by various optimization techniques as in Table III.1. It is apparently seen that the EO finds a minimum operational CHPEED costs of 7117.3067 \$/h that is lower than PSO, IPSO, MPSO, TACPSO, LA, MAO and ASO where they acquired the total function costs (TFC) of 971.4497, 52.0399, 580.7992, 916.3647, 206.859, 1603.9476 and 886.9863\$, respectively.



**FigIII.9:** Convergence Curve of CHPEED Costs.



**FigIII.10:** Run Number of CHPEED Costs.

Other remark, the constraints equalities are verified, that the summation of powers and heats generated is the same of demand, so equal 300 MW and 150 MWth.

Figure III.7 also shows that all the algorithms propose can produce well spread and diverse solutions. Figure III.8 displays the obtained values (best, average, and max values)

among 50 runs of all algorithms technique for the case of minimizing the fuel emission of production.

### **III.6 CONCLUSION AND FUTURE WORK**

The multi-objective economic emission scheduling problem of CHP units is a non-convex, nonlinear, and hard constrained combinatorial problem. This conundrum becomes complex as it deals with two conflicting objectives of fuel cost and the mass of emissions. This work proposes the use of new Meta heuristics algorithms of optimization. The proposed algorithms are tested on different CHPEED case studies.

Our approach solutions obtained by those algorithms are compared with the results available in the literature. For the test system I, the performance improvement in the propose method in saving the fuel costs and reducing the emission levels compared to existing methods. The statistical analysis indicates the quality of the solutions obtained by the proposed method is better than the existing methods. As a result, the PSO, IPSO, MPSO, TACPSO, LA, MAO, EO and ASO methods can be a viable alternative for solving the CHPEED problem and can considerably save fuel cost and reduce emission levels. As future work, the complexity analysis using other algorithms will be carried out and also effective tuning of parameters, sensitivity analysis of the parameters, and its impact on the solution will be analyzed.

## **General conclusion**

CHPDEED model problem of thermal units, CHP and heat only units is a multi-objective optimization problem taking the minimum fuel cost and emission as well as the maximum heat generation, simultaneously.

In this thesis, we propose new metaheuristics algorithms such as PSO, IPSO, MPSO, TACPSO, LA, MAO, EO and ASO to solves non-smooth fuel cost and emission level functions or the combined heat and energy economic dynamic emissions emission (CHPDEED) problem.

After we got the results, we made a comparison of our approach solutions obtained by these algorithms with the results available in the literature. We found that the results obtained were satisfactory in terms of reducing the cost of fuel, reducing emissions and combined heat power significantly.

The ongoing research work is to present a hybridation between the metaheuristics algorithms to consider the cost of Facts systems, the renewable energy source and forced outage rate of generation units as well as considering the voltage stability margin as another objective.

---

## References

- [1]. U.S. Environmental Protection Agency Combined Heat and Power Partnership Fuel and Carbon Dioxide Emissions Savings Calculation Methodology for Combined Heat and Power System. (June 2021)
- [2]. QunNiu 1,\*, Ming You 1 ,Zhile Yang 2 and Yang Zhang 1 Economic Emission Dispatch Considering Renewable Energy Resources—A Multi-Objective Cross Entropy Optimization Approach. (12 May 2021)
- [3]. NnamdiNwulu Combined Heat and Power Dynamic Economic Emissions Dispatch with Valve Point Effects and Incentive Based Demand Response Programs .(2020)
- [4]. VivekK.PatelVimalJ.Savsani.Heat transfer search (HTS): a novel optimization algorithm.( 2015)
- [5].Weiguo Zhao, Liying Wang, Zhenxing Zhang .Atom search optimization and its application to solve a hydrogeologic parameter estimation problem .(2018)
- [6]. JoãoLuizJunho Pereira, Matheus Chuman, Sebastião Simões Cunha Jr and Guilherme Ferreira Gomes. Lichtenberg optimization algorithm applied to crack tip identification in thin plate-like structures. (2020)
- [7]. Suveges, J.M.C. (2014), “Estudoacerca de detecção de danosemestruturas via método de otimização”,Dissertação(MestradoemEngenhariaMecânica),Instituto de EngenhariaMecânica, Universidade Federal de Itajuba, Itajuba
- [8]. YennyVilluendas-Rey 1 , José L. Velázquez-Rodríguez 2 , Mariana Dayanara Alanis-Tamez 2 , Marco-Antonio Moreno-Ibarra 2, and Cornelio Yáñez-Márquez 2,Mexican Axolotl Optimization: A Novel Bioinspired Heuristic. (2021)
- [9]. AfshinFaramarzi a, Mohammad Heidarinejada , Brent Stephens a , SeyedaliMirjalili b,1 .Equilibrium optimizer: A novel optimization algorithm. (2019)
- [10].Jadoun, V. K., Prashanth, G. R., Joshi, S. S., Narayanan, K., Malik, H., & Márquez, F. P. G. (2022). Optimal fuzzy based economic emission dispatch of combined heat and power units using dynamically controlled Whale Optimization Algorithm. Applied Energy, 315, 119033.
- [11].Li, Y., Wang, J., Zhao, D., Li, G., & Chen, C. (2018). A two-stage approach for combined heat and power economic emission dispatch: Combining multi-objective optimization with integrated decision making. Energy, 162, 237-254.
- [12].Basu M. Combined heat and power economic emission dispatch using non dominated sorting genetic algorithm-II. Int J Electr Power Energy Syst 2013; 53(1):135-141.
- [13].Vo, D.H.; Vo, A.T.; Ho, C.M.; Nguyen, H.M. The Role of Renewable Energy, Alternative and Nuclear Energy in Mitigating Carbon Emissions in the CPTPP Countries. Renew. Energy 2020, 161, 278–292.

- [14].Mwasilu, F.; Justo, J.J.; Kim, E.K.; Do, T.D.; Jung, J.W. Electric Vehicles and Smart Grid Interaction: A Review on Vehicle to Grid and Renewable Energy Sources Integration. *Renew. Sustain. Energy Rev.* 2014, 34, 501–516.
- [15].Basu, M. Combined Heat and Power Economic Emission Dispatch Using Non-Dominated Sorting Genetic Algorithm-II. *Int. J. Electron. Power Energy Syst.* 2013, 53, 135–141.
- [16].D. Gong, J. Sun, X. Ji, Evolutionary algorithms with preference polyhedron for interval multi-objective optimization problems, *Inf. Sci.* 233 (2013) 141-161.
- [17].G.C. Maitland, M. Rigby, E.B. Smith, W.A. Wakeham, *Intermolecular forces: their origin and determination.* Clarendon Press, Oxford, 1981.
- [18].C.G. Gray, K.E. Gubbins, *Theory of molecular fluids, Volume 1: fundamentals,* Clarendon Press, Oxford, 1984.
- [19].J.P. Ryckaert, G. Ciccotti, H.J.C. Berendsen, Numerical integration of the cartesian equations of motion of a system with constraints: molecular dynamics of n-alkanes, *J. Comput. Phys.* 23(3) (1977) 327-341.
- [20].Stepinski, T., Uhl, T. and Staszewski, W. (2013), *Advanced Structural Damage Detection: From Theory to Engineering Applications,* John Wiley and Sons. Chichester.

# Abstract



## **Abstract**

The significance and purpose of this multi-objective Combined Heat and Power Economic Emission Dispatch (CHPEED) problem aims to determine the optimal generator output of the co-generation systems, in which two conflicting objectives of the fuel cost and mass of emissions are to be simultaneously minimized. The nonlinear and non convex nature of the objective functions needs a good optimization technique to handle it. This thesis proposes a LA, EO, MAO, ASO, PSO, MPSO and IPSO Optimization Algorithm to solve the multi-objective non-convex MO-CHPEED problem. Both the conflicting objectives of fuel cost and mass of emissions are handled using all algorithms. To highlight the performance of the proposed technique, it is tested on different CHPEED case studies. The results obtained by proposed algorithms compared with latest different published methods show the effectiveness and robustness of the proposed methods for getting better values.

**Key words:** meta-heuristic algorithms, CHPEED, CHP

## **Résumé**

L'importance et le but de ce problème multi-objectifs de dispatching économique des émissions de chaleur et d'électricité combinées (CHPEED) visent à déterminer le rendement optimal du générateur des systèmes de cogénération, dans lequel deux objectifs contradictoires du coût du combustible et de la masse des émissions sont à minimiser simultanément. La nature non linéaire et non convexe des fonctions objectives nécessite une bonne technique d'optimisation pour la gérer. Cette thèse propose un algorithme d'optimisation LA, EO, MAO, ASO, PSO, MPSO et IPSO pour résoudre le problème multi-objectif non convexe MO-CHPEED. Les objectifs contradictoires du coût du carburant et de la masse des émissions sont traités à l'aide de tous les algorithmes. Pour mettre en évidence les performances de la technique proposée, celle-ci est testée sur différentes études de cas CHPEED. Les résultats obtenus par les algorithmes proposés par rapport aux dernières différentes méthodes publiées montrent l'efficacité et la robustesse des méthodes proposées pour obtenir de meilleures valeurs.

**Mots clés :** algorithmes méta-heuristiques, CHPEED, CHP

## ملخص

الهدف من هذه المشكله الرياضيه هو الحصول على الكميات المثلث من ناتج الحرارة والطاقة لوحداث التوليد الملتزمه والتي تتضمن وحدات الطاقة والحرارة فقط ، وذلك باستخدام طرق الاستدلال الفوقي التي تم تعريفها مسبقا: (LA)، (EO)، (MAO)، (ASO)، (PSO)، (MPS) و (IPSO) تستخدم لحل مشكله إرسال الانبعاثات الاقتصديه الديناميكيه للحرارة والطاقة (CHPDEED) ، ويمكن أن تكون الأساليب المقترحة بديلا قابلا للتطبيق لحل مشكله CHPEED ويمكن أن توفر إلى حد كبير تكلفه الوقود وتقلل من مستويات الانبعاثات. كعمل مستقبلي.